

$\eta \rightarrow 3\pi$ at Two Loops In Chiral Perturbation Theory

Johan Bijnens and Karim Ghorbani

*Department of Theoretical Physics, Lund University,
Sölvegatan 14A, S 223-62 Lund, Sweden*

Email: bijnens@thep.lu.se, karim.ghorbani@thep.lu.se

ABSTRACT: We calculate the decay $\eta \rightarrow 3\pi$ at next-to-next-to-leading order or order p^6 in Chiral Perturbation Theory. The corrections are somewhat larger than was indicated by dispersive estimates. We present numerical results for the Dalitz plot parameters, the ratio r of the neutral to charged decay and the total decay rate. In addition we derive an inequality between the slope parameters of the charged and neutral decay. The experimental charged decay rate leads to central values for the isospin breaking quantities $R = 42.2$ and $Q = 23.2$.

KEYWORDS: Chiral Lagrangians, Quark Masses and SM Parameters.

Contents

1. Introduction	1
2. Chiral Perturbation Theory	4
3. Eta decay amplitude: formalism	6
3.1 Matrix-elements in the presence of mixing	6
3.2 Kinematics and isospin	9
3.3 A simplified form for the amplitude to order p^6	10
3.4 Feynman Graphs	11
3.5 Regularization, renormalization and integrals	11
4. Analytical results	12
4.1 Order p^2	12
4.2 Order p^4	12
4.3 Order p^6	13
5. Resonance estimates of the p^6 LECs and the inclusion of the η'	13
6. Numerical results	17
6.1 A first look	17
6.2 Comparison with the dispersive result	20
6.3 Dalitz Plot Parameters	21
6.4 The ratio r and decay rates	25
6.5 Discussion and the values of R and Q	26
7. Conclusions	28
A. A discussion on Dalitzplotparameters and the sign of α	29
B. The order p^4 expression	30
C. The order p^6 LECs dependent part	31

1. Introduction

Since its discovery, the eta particle has been under tense scrutiny, fairly recent reviews are [1, 2]. The eta decay to three pions is particularly interesting. It can only happen due to isospin breaking. This implies that the decay rate vanishes in the limit of equal of up and down quark-masses, ignoring electromagnetic effects. The very first attempts to explain

the decay [3, 4], considering it to undergo electromagnetically, resulted in an almost zero decay rate which was in flat disagreement with experiment.

Later on, a combination of current algebra technique in $SU(3)$ and partially conserved axial-vector current (PCAC) could make a better prediction [5, 6]. This, however, underestimated the observed decay rate by a factor of a few. PCAC and current algebra were generalized into Chiral Perturbation Theory (ChPT) and brought into a modern form [7, 8, 9]. The lowest order for $\eta \rightarrow 3\pi$ was calculated in [5, 6] and the next-to-leading order (NLO) in [10]. The main goal of this paper is to obtain next-to-next-to-leading-order (NNLO) expression for this decay.

We give now a short overview of the present situation, closely following the discussion in [11].

The well-known tree-level result for this decay channel can be derived from current algebra or ChPT and has the structure

$$A(s, t, u) = \frac{B_0(m_u - m_d)}{3\sqrt{3}F_\pi^2} \left(1 + \frac{3(s - s_0)}{m_\eta^2 - m_\pi^2} \right). \quad (1.1)$$

The prefactor $m_u - m_d$ shows that the decay is isospin violating or $SU(2)_V$ -violating. The magnitude of $m_u - m_d$ determines the size of the isospin symmetry breaking coming from the strong interaction itself. A precise determination of this quantity is in principle possible here because its size has a direct impact on the decay rate.

Using Dashen's theorem this factor can be obtained from the physical meson masses by removing electromagnetic effects to lowest order. Following the line of the argument outlined in Dashen's theorem [12] one arrives at

$$B(m_d - m_u) = m_{K^0}^2 - m_{K^+}^2 - m_{\pi^0}^2 + m_{\pi^+}^2. \quad (1.2)$$

Under these circumstances, the theoretical decay width is 66 eV to be compared with 295 eV from experiment [13]. One may consider three potential sources for this discrepancy. First, the violation of the Dashen's theorem due to the electromagnetic interferences increases the value of $m_d - m_u$ [14, 15] and therefore the decay width, but this is not sufficient as will be discussed more in the discussion section. Secondly, electromagnetic corrections of the decay amplitude which are of higher order, order $e^2 p^2$, are safely negligible in comparison with the strong interactions as pointed out in [16] where the analysis of [3, 4] was brought to NLO.

Finally the contribution of the higher order chiral effects must be taken into account. Especially since the strong $\pi\pi$ rescattering in the S -wave channel may develop a significant correction, see e.g. [17, 18]. The NLO corrections were obtained in [10]. The unitarity correction at one-loop level is about half of the total NLO effects. This, of course, confirmed the fact that by virtue of a large eta mass, significant rescattering effects in the S -wave can occur. The vertex corrections and tree graphs make up the rest of the NLO contribution. The coupling constants involved at this level can be rewritten in terms of meson masses except for L_3^r . In [8, 10] L_3^r was estimated by invoking the OZI (Okubo-Zweig-Iizuka) rule and comparing with $\pi\pi$ scattering lengths. Their finding for the decay rate of $\eta \rightarrow 3\pi$ is

160 ± 50 which is still far from the experimental value, however with a large theoretical error.

Given the importance of the unitarity correction at NLO, it was deemed necessary to estimate this part of the corrections to higher order. This can be done using dispersive methods. In [19], extended Khuri-Treiman equations are used to evaluate the two-pion rescattering to the decay $\eta \rightarrow \pi\pi\pi$. They achieve a moderate modification, an increase of about 14% per cent in the amplitude at the center of the Dalitz plot. Moreover, another analysis, based on a somewhat different dispersive method, but also restricting itself to two-pion rescattering, represented in [20] suggests also a mild enhancement to the real part of the amplitude in the physical region. A more model-dependent analysis of dispersive corrections appeared recently [21] relying on combining $U(3) \times U(3)$ ChPT and a relativistic coupled-channels method, finds agreement with data.

Given all these, our motivation to perform a full NNLO computation is twofold. First, due to a relatively large strange quark-mass, the convergence of three-flavour or $SU(3)$ ChPT is an a priori question. The reason hinges on the fact that the ratio $\frac{M_K^2}{M_\rho^2}$ is much larger than $\frac{M_\pi^2}{M_\rho^2}$ and there are possibly large effects as a result of strange quark loops. Three-flavour ChPT is probably less convergent than two-flavour ChPT, see e.g. [22] for a discussion. In general, one needs to have several terms available in order to check convergence. The situation at present is not fully clear, The vector form factor, $K_{\ell 4}$ and $\pi\pi$ -scattering have an acceptable convergence, while we see that for the masses and πK -scattering, the amplitudes seem to converge slower, [23] and references therein. Therefore we would like to check explicitly how far one may pursue on treating the strange quark-mass perturbatively for this particular process, namely $\eta \rightarrow 3\pi$. In addition, at NLO the unitarity correction provided only half of the total correction. It is therefore also of interest to know if the other corrections are important at NNLO as well. This is known to be the case for $K_{\ell 4}$ by comparing [24] and [25].

Our finding shows that the full amplitude up to and including order p^6 corrections converges reasonably acceptably but finds larger corrections than in [19, 20].

In this paper, we perform the full NNLO calculation of $\eta \rightarrow 3\pi$ in standard three-flavour ChPT. We do this to first order in the isospin breaking quantity $m_u - m_d$. In addition, we perform a first numerical analysis with this expression. We have therefore also estimated the order p^6 coupling constants C_i^r , using a resonance chiral Lagrangian, assuming that vector and scalars mesons saturate the C_i^r . In addition, we derive an inequality between the slope parameters.

The layout of this article is as following. In Sect. 2 a brief introduction to Chiral Perturbation Theory is provided. Sect. 3 describes how to calculate the $\eta \rightarrow 3\pi$ amplitude in the presence of mixing, the kinematics for the decay and the form of the amplitude at NNLO. We also show the Feynman diagrams and provides references to how we deal with the loop integrals and renormalization. A short discussion on our analytic results is given in Sect. 4 followed by our estimate of order p^6 low energy constants in Sect. 5. A main part of the manuscript is the numerical results and comparison with experiment given Sect. 6. We first present a discussion on the amplitude level, Sect. 6.1, then compare with

the earlier dispersive results, Sect. 6.2. The main comparison with experiment is done in Sect. 6.3 for the Dalitz plot distributions and in Sect. 6.4 for the ratio of amplitudes. We present the results for the value of R and Q in Sect. 6.5. The App. A contains a discussion on the cancellations inherent in α and the derivation of the inequality between the slope parameters. The remaining appendices present our NLO expression and the dependence on the order p^6 low energy constants.

2. Chiral Perturbation Theory

One approach to address Quantum Chromodynamics (QCD) at low energy is the application of effective field theories. In [26] and references therein some basic concepts and a few interesting examples can be found for this method. As an effective field theory, ChPT is constructed based on the approximate chiral symmetry of the underlying theory (QCD) and is an expansion in external momenta and quark-masses, momenta and meson masses are generically denoted by p and the expansion is in powers of these. The dynamical degree of freedoms i.e. pseudo-Goldstone particles, are manifested as a result of the spontaneous chiral symmetry breaking of QCD. Weinberg [7] systematized the use of effective field theory as an alternative to the current algebra formalism, incorporating naturally the chiral logarithms. Gasser and Leutwyler in two elegant papers presented this expansion including terms of order p^4 and introduced the external field method [8]. They also formulated the extension to three light flavours [9]. They conclude a substantial correction to the $\pi\pi$ scattering lengths and effective ranges at this order. Reviews of ChPT at order p^4 are [27, 28]. This line of work has been further developed to include p^6 corrections, see the review [23]. A more introductory recent review is [29].

The full action consists of subterms with a definite number of derivatives or powers of quark-masses as shown below

$$\mathcal{L}_{eff} = \mathcal{L}_2 + \mathcal{L}_4 + \mathcal{L}_6 + \dots \quad (2.1)$$

The subscript indicates the chiral order. Quark masses are counted as order p^2 using the lowest order relation $m_\pi^2 = B_0 (m_u + m_d)$. The lowest order chiral Lagrangian incorporates two parameters and has the form

$$\mathcal{L}_2 = \frac{F_0^2}{4} \left(\langle D_\mu U D^\mu U^\dagger \rangle + \langle \chi U^\dagger + U \chi^\dagger \rangle \right) \quad (2.2)$$

and the next-to-leading Lagrangian or order p^4 Lagrangian is given as [9]

$$\begin{aligned} \mathcal{L}_4 = & L_1 \langle D_\mu U^\dagger D^\mu U \rangle^2 + L_2 \langle D_\mu U^\dagger D_\nu U \rangle \langle D^\mu U^\dagger D^\nu U \rangle \\ & + L_3 \langle D^\mu U^\dagger D_\mu U D^\nu U^\dagger D_\nu U \rangle + L_4 \langle D^\mu U^\dagger D_\mu U \rangle \langle \chi^\dagger U + U \chi^\dagger \rangle \\ & + L_5 \langle D^\mu U^\dagger D_\mu U (\chi^\dagger U + U^\dagger \chi) \rangle + L_6 \langle \chi^\dagger U + U \chi^\dagger \rangle^2 \\ & + L_7 \langle \chi^\dagger U - U \chi^\dagger \rangle^2 + L_8 \langle \chi^\dagger U \chi^\dagger U + U \chi^\dagger U \chi^\dagger \rangle \\ & - i L_9 \langle F_{\mu\nu}^R D^\mu U D^\nu U^\dagger + F_{\mu\nu}^L D^\mu U^\dagger D^\nu U \rangle \\ & + L_{10} \langle U^\dagger F_{\mu\nu}^R U F^{L\mu\nu} \rangle + H_1 \langle F_{\mu\nu}^R F^{R\mu\nu} + F_{\mu\nu}^L F^{L\mu\nu} \rangle + H_2 \langle \chi^\dagger \chi \rangle. \end{aligned} \quad (2.3)$$

The matrix $U \in SU(3)$ parameterizes the octet of light pseudo-scalar mesons with its exponential representation given in terms of mesonic fields matrix as

$$U(\phi) = \exp(i\sqrt{2}\phi/F_0), \quad (2.4)$$

where

$$\phi(x) = \begin{pmatrix} \frac{\pi_3}{\sqrt{2}} + \frac{\eta_8}{\sqrt{6}} & \pi^+ & K^+ \\ \pi^- & -\frac{\pi_3}{\sqrt{2}} + \frac{\eta_8}{\sqrt{6}} & K^0 \\ K^- & \bar{K}^0 & -\frac{2\eta_8}{\sqrt{6}} \end{pmatrix}. \quad (2.5)$$

The covariant derivative and the field strength tensor are defined as

$$D_\mu U = \partial_\mu U - ir_\mu U + iUl_\mu, \quad F_{\mu\nu}^L = \partial_\mu l_\nu - \partial_\nu l_\mu - i[l_\mu, l_\nu], \quad (2.6)$$

and a similar definition for the right-handed field strength. Here l_μ and r_μ represents the left-handed and right-handed chiral currents respectively. χ is parameterized in terms of scalar (s) and pseudo scalar (p) external densities as $\chi = 2B_0(s + ip)$. In the process discussed in this article we have set $s = \text{diag}(m_u, m_d, m_s)$ and $p = l_\mu = l_\nu = 0$. Finally, the notation $\langle A \rangle = \text{Tr}_F(A)$, the trace over flavours. The $SU(3)$ chiral Lagrangian of order p^6 contains 94 operators. For its explicit terms we refer to [30].

To carry out any practical calculation in a nonrenormalizable effective field theory we need two things. First, a power counting scheme is necessary in order to organize all the contributing operators to the amplitude in a given chiral order. For ChPT this is essentially dimensional counting. The dimensionality of a Feynman graph contributing to the matrix element can be obtained by using the well-known formula[7]

$$D = 2 + 2N_L + \sum_d N_d(d - 2) \quad (2.7)$$

where N_L is the number of loops and N_d is the number of vertices taken from Lagrangian of order d in chiral order. For the implementation of the renormalization program, described below, a dimensional regularization scheme is considered a practical method, particularly when higher order loops are concerned, since it respects chiral symmetry [8] and it only requires one regulator for all loops.

Tree diagrams using only vertices from the Lagrangian \mathcal{L}_2 , provides the lowest order term in the expansion. In general, tree-level diagrams make up the semiclassical part of the unitarity of the S-matrix. We thus ought to include loop effects. The infinities which arise from one loop diagrams with vertices taken from \mathcal{L}_2 can not be absorbed by renormalizing F_0 and B_0 or rescaling the fields since these contribute at tree level at a *different* order in p^2 from the one-loop diagrams. This is the property that characterizes the non-renormalizability of the Lagrangian. The most general Lagrangian at next-to-leading order, \mathcal{L}_4 of (2.3), incorporates 10+2 operators with corresponding low-energy coupling constants (LECs), namely L_i , H_1 and H_2 . The \mathcal{L}_4 provides counterterms polynomial in external momenta and masses which are appropriate for the cancellation of the ultraviolet

divergences of the regularized graphs which show up at one-loop level. We thus split the L_i into an infinite and finite L_i^r part, [7, 8, 9]. By applying the same argument, the construction of the next-to-next-leading Lagrangian is needed in order to extend our calculation to two-loop order. This was carried out in [30]. Renormalization at higher orders contains many subtleties. The procedure used here is discussed extensively in [31, 32]. The full divergence structure at order p^4 [8, 9] and p^6 [32] is known. For our calculation, the cancellation of the divergences is an important cross-check. The nontrivial predictions of ChPT, the so called chiral logarithms, are due to infrared singularities in the chiral limit due to the (pseudo)-Goldstone boson intermediate states. Lattice QCD computations support this logarithmic behavior when compared with ChPT results evaluated in finite volume [33].

The part not determined by ChPT, the L_i^r and higher order LECs, C_i^r at order p^6 , encode the information about higher scale physics which has no dynamical role in our effective field theory and they gain no constraints from the imposed chiral symmetry. They are thus the full freedom allowed by the chiral symmetry Ward identities. For many processes it is turned out that the chiral logarithms do not saturate the amplitude, making the determination of the LECs, an important task. The predictivity of ChPT is limited by the determination of these unknown parameters. Fixing the free parameters in the theory gives rise to a unique low-energy theory for QCD. To this end both theoretical, including Lattice QCD, and phenomenological approaches are needed. Often used is the large N_c limit in the form of Zweig's rule which requires suppression for the NLO LECs $2L_1^r - L_2^r, L_4^r$ and L_6^r . This together with the $\pi\pi$ scattering analysis determine the L_1^r, L_2^r and L_3^r and has been tested in the more accurate determination of these constants from $K_{\ell 4}$. The LECs L_5^r, L_7^r and L_8^r are involved in the higher order corrections to the decay constants, meson masses and Gell-Man-Okubo relation and therefore directly related to quantities which are experimentally obtainable. Moreover, the electromagnetic charge radius of pion and radiative leptonic decay of pion fix the value of L_9^r and L_{10}^r respectively. Detailed discussion on determination of p^4 LECs are given in [9] at order p^6 in [23, 25, 34].

On the other hand, systematic extension to effective field theories incorporating the resonance fields may provide a profound theoretical ground to ultimately underpin the values of the LECs. Resonance field methodology which takes its original form in Sakurai's hypothesis of vector meson dominance. It was worked out at order p^4 by [35]. We will only use it for order p^6 LECs in the simplified form discussed in Sect. 5. More systematic approaches at order p^6 exist [36] but there are also caveats to be observed from short-distance constraints, both positive and negative [37, 38].

3. Eta decay amplitude: formalism

3.1 Matrix-elements in the presence of mixing

In this section we explain how to calculate matrix-elements by the use of the Lehmann-Symanzik-Zimmermann (LSZ) reduction formula in the presence of mixing. This is a generalization of the discussion in [34] Sect. 2, to the case needed here. The scattering amplitude is basically the residue of the Fourier transformed Green function in the limit where all the outgoing particles go on-shell.

For the case of $\eta \rightarrow \pi^+\pi^-\pi^0$, the mixing occurs in the two external legs involving neutral particles pion and eta as illustrated in Fig. 1. For the decay $\eta \rightarrow \pi^0\pi^0\pi^0$ mixing is relevant in all four external legs. In [34] two-point functions were analyzed in all generality as well as amplitudes where one external leg could undergo mixing. Here, we reiterate some basic ingredients introduced there and will lead to derive a general formula that relates the amputated four-point Green function to the scattering amplitude order by order in perturbative expansion of $\eta \rightarrow \pi^+\pi^-\pi^0$. In the ChPT calculation we only retain terms to first order in isospin breaking, we therefore can use the relation (3.20) and do not need a more general formula for $\eta \rightarrow \pi^0\pi^0\pi^0$ to all orders in the mixing.

The amplitude or matrix-element for a process with n ingoing and outgoing particles can be expressed in the form

$$\mathcal{A}_{i_1\dots i_n} = \left(\frac{(-i)^n}{\sqrt{Z_{i_1}\dots Z_{i_n}}} \right) \prod_{i=1}^n \lim_{k_i^2 \rightarrow m_i^2} (k_i^2 - m_i^2) G_{i_1\dots i_n}(k_1, \dots, k_n). \quad (3.1)$$

The function $G_{i_1\dots i_n}(k_1, \dots, k_n)$ is the exact n -point Green function¹ and the coefficients Z_i are defined as

$$G_{ii}(p^2 \approx m_{i\text{phys}}^2) = \frac{iZ_i}{p^2 - m_{i\text{phys}}^2}. \quad (3.2)$$

These are often called field-strength or wave-function renormalization factors.

We begin by decomposing the full four-point function into the amputated four-point function and four full propagators or two-point functions for the external legs.

$$G_{1238} = G_{11}(p^2 \approx m_{1\text{phys}}^2) G_{22}(p^2 \approx m_{2\text{phys}}^2) G_{3i}(p^2 \approx m_{3\text{phys}}^2) G_{8j}(p^2 \approx m_{8\text{phys}}^2) \mathcal{G}_{12ij} \quad (3.3)$$

Subscripts in G_{1238} are designated for the four external particles² namely, π^1, π^2, π^3 and π^8 . A summation over the possible values of i, j is implied in (3.3). Notice that what we observe as particles are those in the physical basis. The numbering in (3.3) and the rest corresponds to the labeling of the fields in the Lagrangian. We express the amputated Green function \mathcal{G}_{12ij} in terms of the contributions at the different chiral orders:

$$\mathcal{G}_{12ij} = \mathcal{G}_{12ij}^{(2)} + \mathcal{G}_{12ij}^{(4)} + \mathcal{G}_{12ij}^{(6)} + \dots \quad (3.4)$$

In view of the fact that only the two fields associated with the neutral pion and eta particles mix, the relevant two-point functions G_{ij} constitute a two-by-two matrix $G = (G_{ij})$ with $i, j = 3, 8$. This can be done since the only nonzero off-diagonal elements are $G_{38} = G_{83}$. For this matrix we define $G^{-1} = -i\mathcal{P}$ and \mathcal{P} can be written as $\mathcal{P} = P^{-1} + \Pi$. $P^{-1} = \text{diag}(p^2 - m_{i0}^2)$ is the matrix of (inverse) lowest order propagators. We *assume* here

¹We consider as operators that are in the Green functions the fields as present in the Lagrangian. The formula is valid for all operators with a nonzero coupling to single-particle states.

²We use a somewhat generic notation here, 1,2 for the nonmixing external legs and 3,8 for the mixing external legs corresponding to π^0 and η .

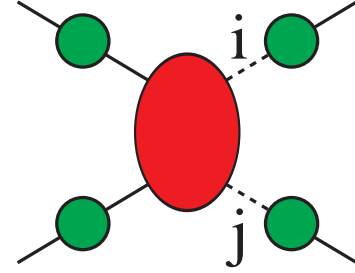


Figure 1: The full four-point Green function is represented. The Oval stands for the amputated four-point Green function and circles indicate the full two-point functions. The solid lines are external mesons and the dashed lines labeled by i and j , indicate the sum over states implied in the two external legs where mixing occurs.

$$\begin{aligned}
& + \frac{1}{2} \left(Z_{33}^{(4)} \frac{\Pi_{38}(3)^{(4)}}{\Delta m_1^2} + Z_{88}^{(4)} \frac{\Pi_{38}(3)^{(4)}}{\Delta m_1^2} + Z_{11}^{(4)} \frac{\Pi_{38}(3)^{(4)}}{\Delta m_1^2} \right) \mathcal{G}_{1288}^{(2)} \\
& + \frac{1}{2} \left(Z_{33}^{(4)} \frac{\Pi_{38}(8)^{(4)}}{\Delta m_2^2} + Z_{88}^{(4)} \frac{\Pi_{38}(8)^{(4)}}{\Delta m_2^2} + Z_{11}^{(4)} \frac{\Pi_{38}(8)^{(4)}}{\Delta m_2^2} \right) \mathcal{G}_{1233}^{(2)}. \tag{3.12}
\end{aligned}$$

We defined the abbreviations $\Delta m_1^2 = m_\pi^2 - m_{\eta_0}^2$ and $\Delta m_2^2 = m_\eta^2 - m_{\pi_0}^2$ with first a physical mass and the second term the lowest order mass. $\Pi_{ij}^{(k)}(I)$ are evaluated at the physical π^0 mass for $I = 3$ and at the physical η mass for $I = 8$. The $\mathcal{G}_{12ij}^{(n)}$ are evaluated at the physical charged pion mass for the legs with indices 1 or 2 and at the physical π^0 mass for the leg labeled i and at the physical η mass at the leg labeled j . The set of terms are shown at the different orders.

3.2 Kinematics and isospin

We write the amplitude for the decay $\eta(p_\eta) \rightarrow \pi^+(p_+)\pi^-(p_-)\pi^0(p_0)$ using the Mandelstam variables

$$\begin{aligned}
s &= (p_+ + p_-)^2 = (p_\eta - p_0)^2, \\
t &= (p_+ + p_0)^2 = (p_\eta - p_-)^2, \\
u &= (p_- + p_0)^2 = (p_\eta - p_+)^2. \tag{3.13}
\end{aligned}$$

These are linearly dependent

$$s + t + u = m_{\pi^0}^2 + m_{\pi^-}^2 + m_{\pi^+}^2 + m_\eta^2 \equiv 3s_0. \tag{3.14}$$

Due to the $SU(2)_V$ symmetry breaking the isospin basis and physical basis in the π^0 - η subset do not coincide. To diagonalize the mass matrix and consequently the two-point functions at *leading order* we perform the following transformation and find the corresponding *lowest order* mixing angle

$$\begin{aligned}
\pi_3 &= \pi \cos(\epsilon) - \eta \sin(\epsilon) \\
\eta_8 &= \pi \sin(\epsilon) + \eta \cos(\epsilon) \tag{3.15}
\end{aligned}$$

The lowest order mixing angle is

$$\begin{aligned}
\tan(2\epsilon) &= \frac{\sqrt{3}}{2} \frac{m_d - m_u}{m_s - \hat{m}}, \\
\hat{m} &= (m_u + m_d)/2. \tag{3.16}
\end{aligned}$$

G-parity requires the amplitude to vanish at the limit $m_u = m_d$ and therefore it must inevitably be accompanied by an overall factor of $m_u - m_d$ which we have chosen to be in the form of $\sin(\epsilon)$.

$$A(\eta \rightarrow \pi^+ \pi^- \pi^0) = \sin(\epsilon) M(s, t, u) \tag{3.17}$$

Since the amplitude is invariant under charge conjugation we have

$$M(s, t, u) = M(s, u, t). \tag{3.18}$$

Note that the isospin breaking factor which is pulled out is different in different references, [10] and [39] use different quantities. We have chosen $\sin(\epsilon)$ since it is the factor that naturally shows up at lowest order.

For the eta decay to three neutral pions, the amplitude must be symmetric under the exchange of pions (Bose symmetry) and this together with isospin symmetry and using the fact that the decay is caused by the $\Delta I = 1$ operator $(1/2)(m_u - m_d)(\bar{u}u - \bar{d}d)$ implies

$$A(\eta \rightarrow \pi^0 \pi^0 \pi^0) = \sin(\epsilon) \overline{M}(s, t, u) \quad (3.19)$$

with

$$\overline{M}(s, t, u) = M(s, t, u) + M(t, u, s) + M(u, s, t). \quad (3.20)$$

This relation is only true when isospin breaking in the amplitude is taking into account to first order only. $M(s, t, u)$ and $\overline{M}(s, t, u)$ are treated in the isospin limit. We will work in this limit in the remainder of the paper.

3.3 A simplified form for the amplitude to order p^6

The scattering amplitude can be represented in terms of components with definite isospin assignments as[20]

$$M(s, t, u) = M_0(s) + (s - u)M_1(t) + (s - t)M_1(u) + M_2(t) + M_2(u) - \frac{2}{3}M_2(s). \quad (3.21)$$

The function $M_I(x = s, t, u)$ indicates scattering in the kinematic x -channel with total isospin I . The derivation relies on the axioms such as analyticity, unitarity and crossing symmetry imposed on the S-matrix, gives rise to this exceptionally useful representation. For the derivation and detailed discussion for the case of $\pi\pi$ we refer to [40]. This relation only holds up to $\mathcal{O}(p^8)$.

The argument is based on the fact that nonpolynomial dependence on s, t, u is related to an absorptive part via unitarity. Up to order p^6 there are only absorptive parts in the two-pion S and P -waves and then using isospin one derives the form (3.21).

It is important to note that the polynomial part of the amplitude cannot be split uniquely into M_I functions since the relation $s + t + u = 3s_0$ allows a different redistribution of the said part to the M_I s. A list of the equivalent redefinitions for the case of $K \rightarrow 3\pi$ can be found in App. A of [41]. The choice we made is to remove as much as possible first out of M_2 and then out of M_1 .

Eq. (3.21) makes the formidable task of handling two loop expressions much more manageable and we indeed confirmed explicitly the validity of Eq. (3.21) for the decay $\eta \rightarrow \pi^0 \pi^+ \pi^-$ at $\mathcal{O}(p^6)$.

Note that the neutral decay amplitude can also be expressed directly in terms of the $M_I(t)$,

$$\overline{M}(s, t, u) = M_0(s) + M_0(t) + M_0(u) + \frac{4}{3}(M_2(s) + M_2(t) + M_2(u)). \quad (3.22)$$

when using the isospin relation (3.20).

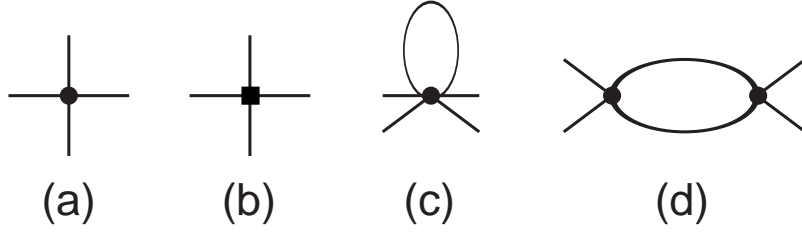


Figure 2: The Feynman diagrams of order p^2 , (a) and of order p^4 , (b)-(d).

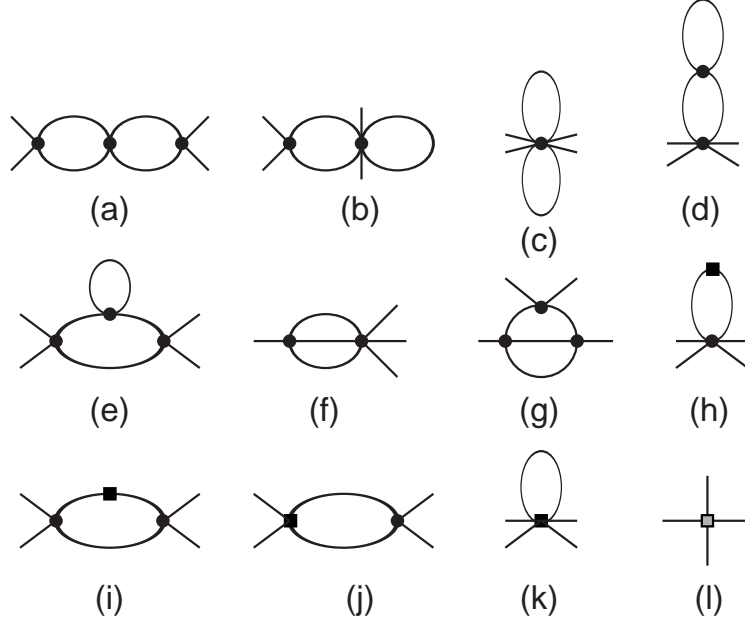


Figure 3: Feynman diagrams of order p^6 .

3.4 Feynman Graphs

We have collected all the amputated Feynman diagrams needed for this process according to the ChPT power counting scheme introduced in Sect. 2. In these figures a filled circle denotes a vertex of order p^2 , a filled square a vertex of order p^4 and the grey filled square a vertex of order p^6 .

3.5 Regularization, renormalization and integrals

As a regularization method we use dimensional integration. The regularization method is described in detail in [31, 32].

The one-loop functions needed are defined in many places. We use the definitions as given in [42, 25, 43]. The two-loop integrals we evaluate numerically using the methods described in [42] for the sunset integrals and in [43] for the vertex integrals.

In addition to the integrals given there, we also need derivatives w.r.t. one of the masses in order to be able to pull out the overall isospin breaking factor in the amplitudes. For all the one-loop integrals needed, these derivatives can be derived exactly. An example

of a relation we derived, needed to obtain agreement with the order p^4 result of [10] is

$$\begin{aligned}\overline{C}(m^2, m^2, m^2, p^2) &= \frac{\partial}{\partial m_1^2} \overline{B}(m_1^2, m_2^2, p^2) \Big|_{m_1^2=m_2^2=m^2} \\ &= -\frac{2}{p^2 - 4m^2} \left(\overline{B}(m^2, m^2, p^2) - \overline{B}(m^2, m^2, 0) - \frac{2}{16\pi^2} \right). \quad (3.23)\end{aligned}$$

For the two-loop integrals, we have taken the derivatives numerically.

4. Analytical results

4.1 Order p^2

At leading order there is one tree graph from \mathcal{L}_2 to compute since we have already diagonalized the fields in the lowest order Lagrangian. The lowest order decay amplitude takes on the form

$$M^{(2)}(s) = \frac{1}{F_\pi^2} \left(\frac{4}{3} m_\pi^2 - s \right) \quad (4.1)$$

using the identity $s + t + u = 3s_0$. F_π and m_π are the physical pion decay constant and the physical pion mass respectively, which involve corrections of order p^4 and p^6 . The higher order corrections due to the redefinition of the parameters are carried to the respective amplitude of order p^4 and p^6 . This agrees with the known lowest order results [5, 6, 10] but is written in a somewhat different form. We have chosen this form since it brings out the Adler zero explicitly.

4.2 Order p^4

At this order we obtain vertices from \mathcal{L}_2 to construct the tadpole, Fig. 2(c) and the so-called unitarity graphs Fig. 2(d) and in addition, the tree diagram from \mathcal{L}_4 , Fig. 2(b). These are the diagrams contributing to $\mathcal{G}_{1238}^{(4)}$ of (3.11). The second set of terms in $\mathcal{A}_{1238}^{(4)}$ in (3.11) is from what is usually called wave function renormalization. The final two terms in $\mathcal{A}_{1238}^{(4)}$ of (3.9) are what are called the mixing corrections³.

The sum of all the contributions described in Eq. (3.11) gives the full one-loop amplitude. G-parity requires the amplitude to be proportional to $\sin(\epsilon)$ as was the case at leading order. This does not occur explicitly at order p^4 , because now isospin is broken in the meson loops. In order to pull out an overall mixing angle we then carry out a Taylor expansion of the loop integrals involving two charged kaons around the neutral kaon mass. The amplitude is written as

$$\begin{aligned}M^{(4)}(s, t, u) &= \frac{1}{F_\pi^4} \left[M_0^{(4)}(s) + (s - u)M_1^{(4)}(t) + (s - t)M_1^{(4)}(u) + M_2^{(4)}(t) + M_2^{(4)}(u) \right. \\ &\quad \left. - \frac{2}{3}M_2^{(4)}(s) \right]. \quad (4.2)\end{aligned}$$

³In our calculations, lowest order mixing is dealt with exactly. The mixing at higher orders is dealt with perturbatively.

The full expression at $\mathcal{O}(p^4)$ for the $M^{(4)}(t)$ can be found in App. B. There, all the masses and the pion decay constant are the physical ones. We have taken the expressions at lowest order and one-loop order and added the correction terms needed at the higher orders to bring them into the form we show in (4.1) and App. B. and are corrected up to order p^6 . We retain all the p^4 effective constants in our expression, in contrast to [10] where all but L_3 are eliminated in favor of measurable quantities. We have also found our analytical results in full accord with that in [10].

4.3 Order p^6

We again split the amplitude as in (3.21).

$$M^{(6)}(s, t, u) = \frac{1}{F_\pi^6} \left[M_0^{(6)}(s) + (s - u)M_1^{(6)}(t) + (s - t)M_1^{(6)}(u) + M_2^{(6)}(t) + M_2^{(6)}(u) - \frac{2}{3}M_2^{(6)}(s) \right]. \quad (4.3)$$

However, the order p^6 expression is extremely long. The dependence on the order p^6 LECs is given in App. C. We split the result in several parts

$$M_I^{(6)}(t) = M_I^C(t) + M_I^{LL}(t) + M_I^T(t). \quad (4.4)$$

$M_I^C(t)$ contains the contributions from the order p^6 LECs, $M_I^{LL}(t)$ contains the contributions that involve the order p^4 LECs and $M_I^T(t)$ is the pure two-loop contribution, only dependent on the masses of the pseudoscalars. $M_I^T(t)$ itself we split in the parts coming from vertex-integrals, sunset-integrals and the rest. The latter split is definitely not unique. It depends on how many of the relations between the various integrals are actually used and we observe strong numerical cancellations between its different parts. We therefore only quote numerical results for $M_I^T(t)$ as a whole.

The calculation has been performed independently by each of the authors, the divergences agree with those of the general calculation [32] and nonlocal divergences cancel as required. We have also checked explicitly that the amplitudes can be brought into the form (3.21). The numerical results are also done twice and we have checked that they agree. Finally, μ -independence has been checked numerically and found to be satisfactory. The latter is not exact, since we have expressed the order p^4 and p^6 in the physical masses and there is a residual $p^8 \mu$ dependence left over. We do observe a strong cancellation between the order p^4 and $p^6 \mu$ -dependence as expected.

5. Resonance estimates of the p^6 LECs and the inclusion of the η'

Chiral symmetry imposes no constraints on the values of the low energy constants, nevertheless these constants do depend on the parameters of the underlying theory, QCD, namely the masses of the heavy quarks and the scale Λ_{QCD} . Hence, all the LECs may be determined from first principles employing the Lattice QCD technique. At order p^4 , most of the LECs have been determined phenomenologically and some of them are checked

numerically by the use of the Lattice QCD [44]. At the present time, only very few of the order p^6 LECs are estimated using available data[23]. In this section, we will discuss briefly how to do an approximate estimation of the LECs within the framework of the resonance effective field theories. In the limit $N_c \rightarrow \infty$, the matching of the QCD and ChPT might become feasible since now, an infinite tower of massive narrow hadronic states emerge. With these states one can construct a chiral invariant Lagrangian incorporating both Goldstone mesons and resonance fields. In practice one has to do a truncation on the hadronic spectrum and limit the resonance multiplets to low-lying excitations. The construction of the p^4 resonance Lagrangian is discussed in the pioneering works[35, 37]. The extension of the earlier works to $\mathcal{O}(p^6)$ is presented in [36]. In the following we present a resonance Lagrangian at order p^6 with the vector realization of the vector fields, [35, 36] use the antisymmetric tensor formulation. The exchange of axialvector resonances does not contribute to the process $\eta \rightarrow 3\pi$ and they are not discussed here. We do in addition to the lowest vector nonet include the pseudoscalar singlet and a scalar nonet.

The building blocks one needs for the construction of the Lagrangian take the form

$$\begin{aligned} u^\mu &= iu^\dagger D^\mu U u^\dagger \quad \text{with} \quad u^2 = U, \\ \chi_\pm &= u^\dagger \chi u^\dagger \pm u \chi^\dagger u. \end{aligned} \quad (5.1)$$

These transform as an octet under $SU(3)_V$ using the general CCWZ construction⁴.

The resonance fields are counted as order 1 in the chiral counting. We do not include the complete possible list of terms here but restrict to a smaller subset which contains the lowest order interactions of the resonances in our chosen representation for them. This is the same subset of possible terms used in most of the work on NNLO ChPT. We only show the terms relevant for $\eta \rightarrow 3\pi$ here. For the vector fields we use as Lagrangian

$$\mathcal{L}_V = -\frac{1}{4}\langle V_{\mu\nu} V^{\mu\nu} \rangle + \frac{1}{2}m_V^2 \langle V_\mu V^\mu \rangle - \frac{ig_V}{2\sqrt{2}} \langle V_{\mu\nu} [u^\mu, u^\nu] \rangle + f_\chi \langle V_\mu [u^\mu, \chi_-] \rangle. \quad (5.2)$$

$V_{\mu\nu} = \nabla_\mu V_\nu - \nabla_\nu V_\mu$ and the matrix content of the vector field reads in terms of the more familiar observed particles

$$V_\mu = \begin{pmatrix} \frac{\rho^0}{\sqrt{2}} + \frac{\omega}{\sqrt{2}} & \rho^+ & K^{*+} \\ \rho^- & -\frac{\rho^0}{\sqrt{2}} + \frac{\omega}{\sqrt{2}} & K^{*0} \\ K^{*-} & \bar{K}^{*0} & \phi \end{pmatrix}_\mu. \quad (5.3)$$

The singlet component does not contribute to order p^6 for $\eta \rightarrow 3\pi$. For the scalar meson nonet, the matrix of fields S , we consider

$$\mathcal{L}_S = \frac{1}{2} \langle \nabla^\mu S \nabla_\mu S - M_S^2 S^2 \rangle + c_d \langle S u^\mu u_\mu \rangle + c_m \langle S \chi_+ \rangle \quad (5.4)$$

At tree level integrating out the heavy fields is equivalent to applying the equation of motion for the elimination of the heavy fields. To solve the equation of motion we perform

⁴See Refs. [35, 36] for a more extensive discussion and references

a perturbative expansion of the resonance field with coefficients in increasing powers of $1/M_R$ (M_R , the resonance mass) and then solve the equation of motion recursively. We obtain for the Vector V^μ and Scalar S resonance field

$$\begin{aligned} V^\mu &= -\frac{ig_V}{\sqrt{2}M_V^2}\nabla_\nu[u^\nu, u^\mu] - \frac{1}{M_V^2}f_\chi[u^\mu, \chi_-] + \dots \\ S &= \frac{c_d}{M_S^2}(u_\mu u^\mu) + \frac{c_m}{M_S^2}(\chi_+) + \frac{c_d}{2M_S^4}\nabla^\nu\nabla_\nu(u_\mu u^\mu) + \frac{c_m}{2M_S^4}(\nabla^\mu\nabla_\mu\chi_+) + \dots \end{aligned} \quad (5.5)$$

Substitution of (5.5) in the Lagrangians (5.2) and (5.4) we obtain the effective action from V, S -exchange[31, 25]

$$\mathcal{L}_V = -\frac{1}{4M_V^2}\left\langle\left(ig_V\nabla_\mu[u^\nu, u^\mu] - f_\chi\sqrt{2}[u^\nu, \chi_-]\right)^2\right\rangle \quad (5.6)$$

$$\mathcal{L}_S = \frac{1}{2M_S^4}\left\langle(c_d\nabla^\nu(u_\mu u^\mu) + c_m\nabla^\nu\chi_+)^2\right\rangle \quad (5.7)$$

The resonance couplings were determined in [31, 25, 35]. The values we use are

$$f_\chi = -0.025, \quad g_V = 0.09, \quad c_m = 42 \text{ MeV}, \quad c_d = 32 \text{ MeV}, \quad (5.8)$$

and for the masses we use

$$m_V = m_\rho = 0.77 \text{ GeV}, m_S = 0.98 \text{ GeV}. \quad (5.9)$$

The η' plays a significant role in processes involving η due to the $\eta - \eta'$ mixing. Within the quark model, η' and η mix because of the $SU(3)$ symmetry breaking. In the chiral limit the pseudoscalar octet becomes massless but the η' has a residual mass as a result of the axial $U(1)$ anomaly. In the combined chiral and large N_c limit, however, a nonet of Goldstone particles emerge and this provides a perturbative framework to investigate the dynamical interplay between η' and Goldstone particles, see e.g. [45, 46].

One important result is the saturation of the low energy constant L_7 by the η' exchange[9]

$$L_7^{\eta'} = -\frac{\tilde{d}_m^2}{2M_{\eta'}^2} \quad (5.10)$$

We therefore perceive the η' dynamical interferences at order p^4 through its contribution to the effective constant L_7 . In the light of this realization, the $\eta - \eta'$ mixing effect on the C_i involved in the decay $\eta \rightarrow 3\pi$ can be obtained by constructing an appropriate $U(3)$ Lagrangian at order p^6 . That $\eta - \eta'$ mixing can be treated perturbatively for the decay $\eta \rightarrow 3\pi$ is discussed extensively in [45]. We take for the singlet degree of freedom P_1 the simple Lagrangian

$$\mathcal{L}_{\eta'} = \frac{1}{2}\partial_\mu P_1 \partial^\mu P_1 - \frac{1}{2}M_{\eta'}^2 P_1^2 + i\tilde{d}_m P_1 \langle \chi_- \rangle. \quad (5.11)$$

Integrating out P_1 leads to the order p^4 term with L_7 of (5.10) and the order p^6 Lagrangian

$$\mathcal{L}_{\eta'} = -\frac{\tilde{d}_m^2}{2M_{\eta'}^4}\partial_\mu \langle \chi_- \rangle \partial^\mu \langle \chi_- \rangle \text{ with } \tilde{d}_m = 20 \text{ MeV}. \quad (5.12)$$

i	$\frac{F_0^2 g_V^2}{M_V^2}$	$\frac{F_0^2 g_V f_\chi}{\sqrt{2} M_V^2}$	$\frac{F_0^2 f_\chi^2}{M_V^2}$	$\frac{F_0^2 c_d^2}{M_S^4}$	$\frac{F_0^2 c_d c_m}{M_S^4}$	$\frac{F_0^2 c_m^2}{M_S^4}$	$\frac{F_0^2 d_m^2}{M_{P_1}^4}$
1	1/8			-1/4			
4	1/8						
5					1/2		
8					1/2		
10					-1		
12					-1/2		
18							-1/2
19					1/27		-1/9
20					-1/18		1/6
22	1/16	1/2		1/8			
24	1/12			-1/6			
25	-3/8	-1		1/4			
26	7/36	1	1	-5/36	-1/2	-1/4	
27	-1/36			1/18	1/3		-1
28	1/72			-1/36			
29	-11/72	-1	-1	1/18	-1/2	-1/4	
31					-7/18		-1/3
32					-1/18		1/6
33					2/9		-1/6

Table 1: The resonance exchange estimates of C_i contributing to $\eta \rightarrow 3\pi$. The vector exchange results are taken from [48] scalar exchange from [36]. For the singlet eta contribution, see text. The result for the C_i^r is the top row multiplied by the coefficients given in the table. Only nonzero coefficients that also contribute to $\eta \rightarrow 3\pi$ are given. We use here the dimensionless version of the C_i^r . Only terms relevant for $\eta \rightarrow 3\pi$ are shown.

The latter can be rewritten in general in terms of the basis of operators of [30]. The result is⁵

$$\begin{aligned}
\partial_\mu \langle \chi_- \rangle \partial_\mu \langle \chi_- \rangle = & O_{18} + \frac{2}{9} O_{19} - \frac{1}{3} O_{20} + \frac{1}{3} O_{21} + 2O_{27} + \frac{2}{3} O_{31} - \frac{1}{3} O_{32} + \frac{1}{3} O_{33} \\
& - 2O_{35} + O_{37} - \frac{8}{3} O_{94}.
\end{aligned} \tag{5.13}$$

We have derived the contribution to $\eta \rightarrow 3\pi$ in different ways. An option is to evaluate explicitly the resonance exchange directly from the Lagrangians with resonances. The second method is as described above, to evaluate the exchange in general in terms of an effective Lagrangian of the pseudoscalars only and then calculate with that one. The third option is to rewrite the contributions from vector and resonance exchange in terms of the order p^6 ChPT Lagrangian [32]. The latter can be done for the scalar octet using the results of [36], for the vector nonet using [48] and the pseudoscalar singlet using (5.13). We

⁵This was derived by the authors of [25] but not included in the final manuscript. It agrees with the expression shown by Kaiser[47].

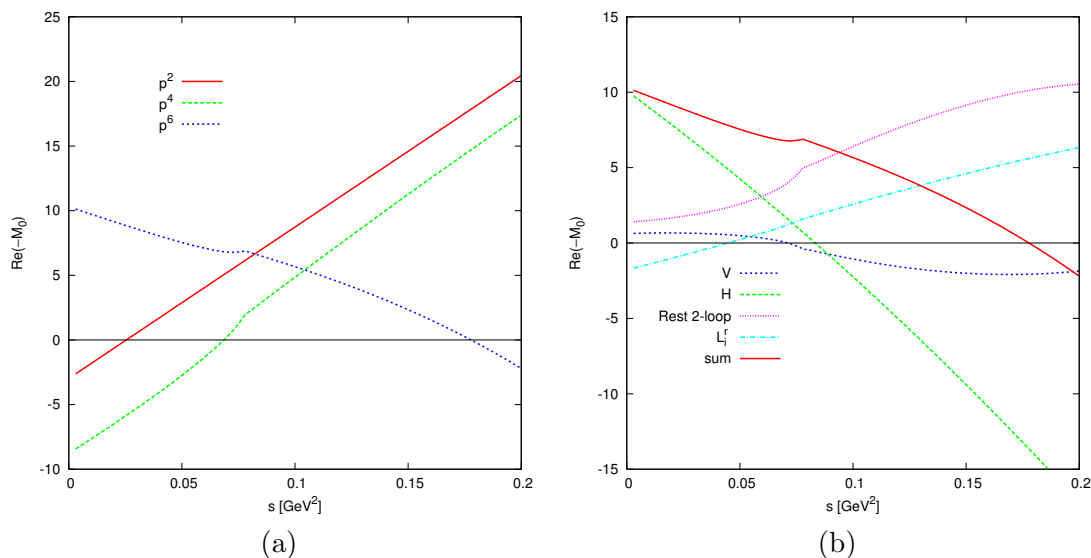


Figure 4: (a) The order p^2 , p^4 and p^6 contribution to $-\text{Re}M_0(s)$. (b) The order p^6 contribution to $-M_0(t)$ split into its parts, the contribution from vertex-integrals (V), sunsetintegrals (H) and the remaining pure two-loop part as well as the L_i^r -dependent part.

have checked that the first method also gives the Lagrangians (5.6) and (5.7) and that the 2nd and third method in the end give the same contribution to $\eta \rightarrow 3\pi$. The results for the C_i are quoted in Tab. 1. In the numerical estimates we have used $F_0 = F_\pi$.

6. Numerical results

6.1 A first look

In this section we present some plots of the amplitude to give a first impression of how the higher orders look like. We start with figures showing different contributions to $M_{0,1,2}(s)$. It should be noted that since terms can be moved around between the $M_I(s)$ these figures cannot be used to check whether we have convergence or not. They are shown for illustration only. We have actually plotted the negative of the quantities defined earlier, this makes the size of the corrections easier to judge.

The input values we use are the physical eta mass, $m_\eta = 54.3$ MeV, the average Kaon mass removing electromagnetic effects, $m_K = 494.53$ MeV and a pion mass such that $s + t + u = m_\eta^2 + 3m_\pi^2$ is satisfied for the charged and neutral decay. So we use $3m_\pi^2 = 2m_{\pi^+}^2 + m_{\pi^0}^2$ for the charged decay and $m_\pi^2 = m_{\pi^0}^2$ for the neutral decay. More general plots were always done with the mass as for the charged decay. The order p^4 LECs are set to the values for fit 10 of [34] and we have set the order p^6 LECs equal to zero. The subtraction scale is $\mu = 770$ MeV.

In Fig. 4(a) we show the contributions of order p^2 , p^4 and p^6 to $M_0(t)$. One sees an acceptable convergence in the physical domain for the decay. In Fig. 4(b) we show how the different parts contribute. As one can see, there are sizable cancellations in the order p^6 contribution. In Fig. 5(a) we show the various contribution to the absorptive part of

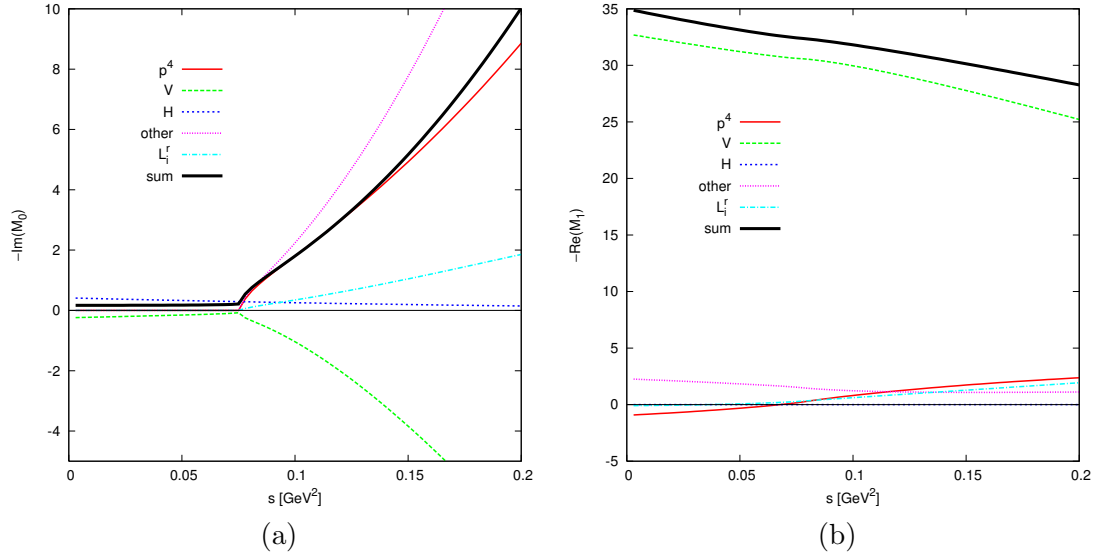


Figure 5: (a) The order p^2 , p^4 and p^6 contribution to $-\text{Im}M_0(s)$. (b) The order p^4 and p^6 contribution to $-\text{Re}M_1(s)$.

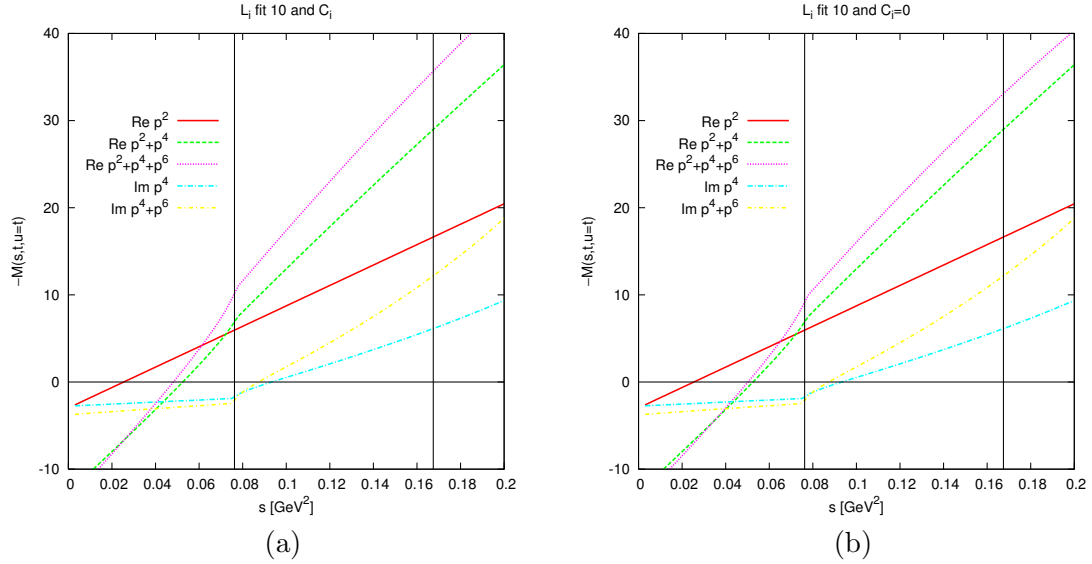


Figure 6: The amplitude $M(s, t, u)$ along the line $t = u$. The vertical lines indicate the physical region. (a) Shown are the real and imaginary parts with all parts summed up to the given order. (b) Same plot but the contribution from the C_i^r has been removed.

$M_0(s)$. We see that the total p^6 is about the same size as the order p^4 one. To be noted is the three particle cut that contributes first at order p^6 . This allowed $M_0(s)$ to have an absorptive part also below the two-pion threshold. This cut gets contributions from the vertex- and the sunset-integrals, diagrams in Fig. 3(f) and (g). As expected, this cut gives a rather small contribution. We also show a case where the convergence looks bad, $M_1(s)$ shown in Fig. 5(b). When we look at the full amplitude this large correction is not visible.

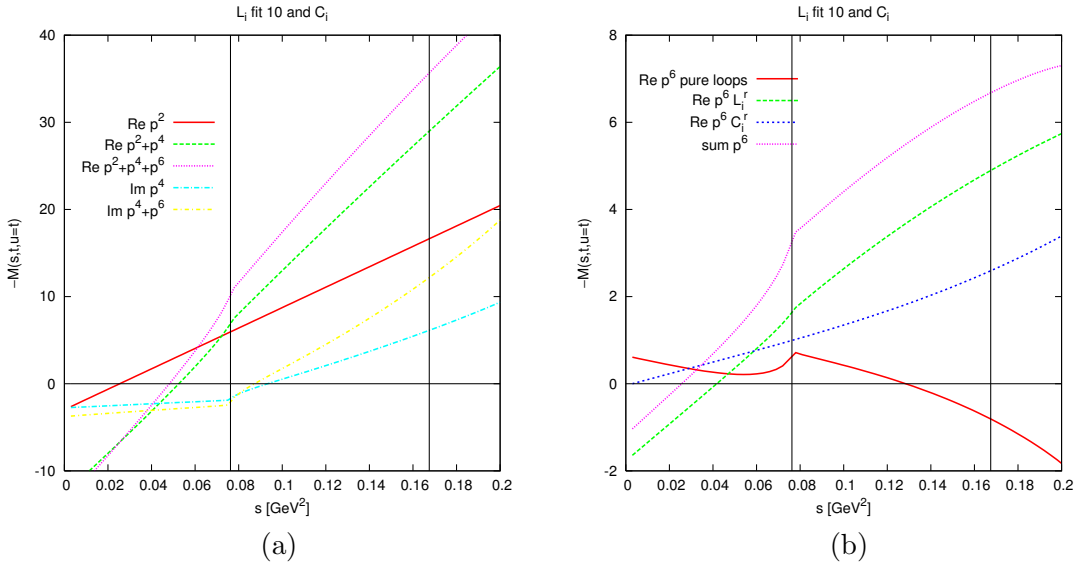


Figure 7: The amplitude $M(s, t, u)$ along the line $t = u$. The vertical lines indicate the physical region. (a) Shown are the real and imaginary parts with all parts summed up to the given order but the contribution from the L_i^r and C_i^r have been removed. (b) Same plot but showing the various parts.

It seems to be tempered sufficiently when all the different $M_I(s)$ are summed as in (3.21).

To see this, let us look at the amplitude along the line $u = t$ as a function of s for the full amplitude. Here we plot first our full result. In Fig. 6 we show the order p^2 , the sum of order p^2 and p^4 and finally the sum of order p^2 , p^4 and order p^6 . Note the shift in the Adler zero in going from order p^2 to order p^4 .

As a final part here we show the dependence on the subtraction constant μ . As mentioned above, our full result is μ -independent to the order it should be with a cancellation between the variation at NLO and NNLO. The μ -dependence creeps in via the estimate of the C_i^r and at which scale μ it is applied. In Fig. 8 we plot the real part of the amplitude to NLO and NNLO at $\mu = 0.6$, 0.77 and 0.9 GeV. The variation with μ is fairly small.

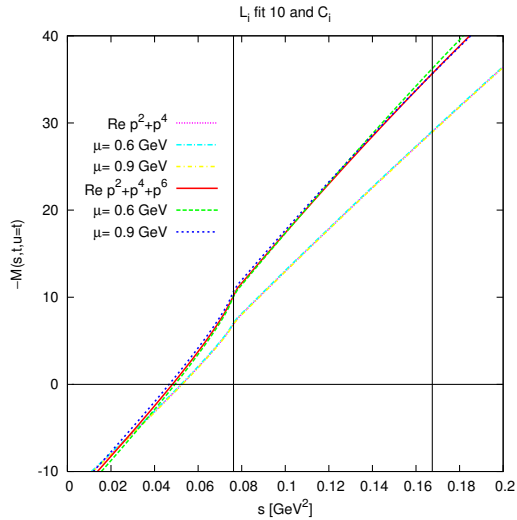


Figure 8: The amplitude $M(s, t, u)$ along the line $t = u$ to NLO and NNLO order for three choices of the subtraction point μ , i.e. three choices at which the estimate of the $C_i^r(\mu)$ is applied.

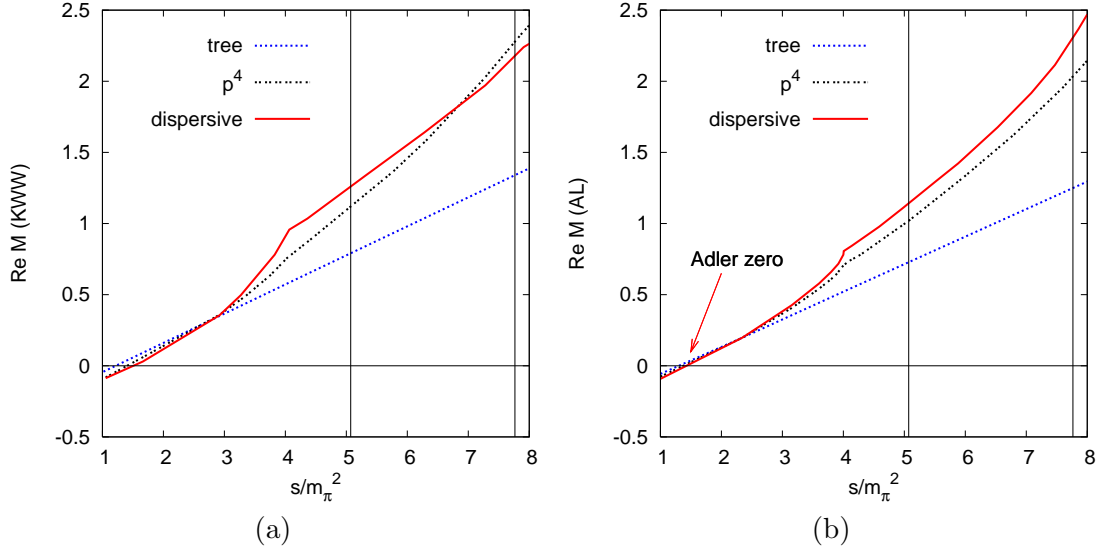


Figure 9: (a) Decay amplitude obtained by use of extended Khuri-Treiman equations[19] along the line $s = u$. (b) Alternative dispersive analysis for the decay amplitude[20]. Figs. from [49], adapted from [19, 20].

6.2 Comparison with the dispersive result

Since long ago it has been known that the decay amplitude of $\eta \rightarrow \pi\pi\pi$ accepts a sizable enhancement due to the loop correction at $\mathcal{O}(p^4)$ [10]. In fact it turned out that a large part of this correction comes from $\pi\pi$ rescattering in the final state as expected[17, 18]. This has prompted two different analyses using dispersive methods. They both restrict themselves to $\pi\pi$ -rescattering but differ in how the subtraction constants are determined and in how the dispersion theory is used. Ref. [19] used the Khuri-Treiman equations and fixed the subtraction constants by comparing with the one-loop expression at various kinematical points. Ref. [20] generalized the reasoning behind [40] to obtain a series of dispersion relations for the $M_I(t)$ defined in (3.21). Their predictions on the decay width are in agreement within the quoted uncertainties, [20] finds $\Gamma = 219 \pm 22$ eV and [19] obtain $\Gamma = 209 \pm 20$ eV. Both used Dashen's theorem and the then known value of L_3^r to fix the overall constant. These, however, must be compared with $\Gamma_{exp} = 295$ eV which provides a check on Dashen's theorem [39]. On the other hand, as emphasized in [11, 49], they have a rather different behaviour in the phasespace distributions. This is shown in Fig. 9. It can be seen that the slope for [19] is smaller than the order p^4 results while [20] has a larger slope than the one-loop result. The latter also follows from the very simplified dispersive analysis performed in [11] shown in Fig. 10(a). The general feature of the result of [20] seems to be robust against small changes. One motivation for the present work is to check these predictions and see if other effects could be important as well, at order p^4 only about half the correction came from the unitarity correction.

We can now compare the same plot coming from our full NNLO calculation shown in Fig. 10(b). The total order p^6 correction is somewhat larger than observed in [19, 20] but the trend is definitely in better agreement with [20].

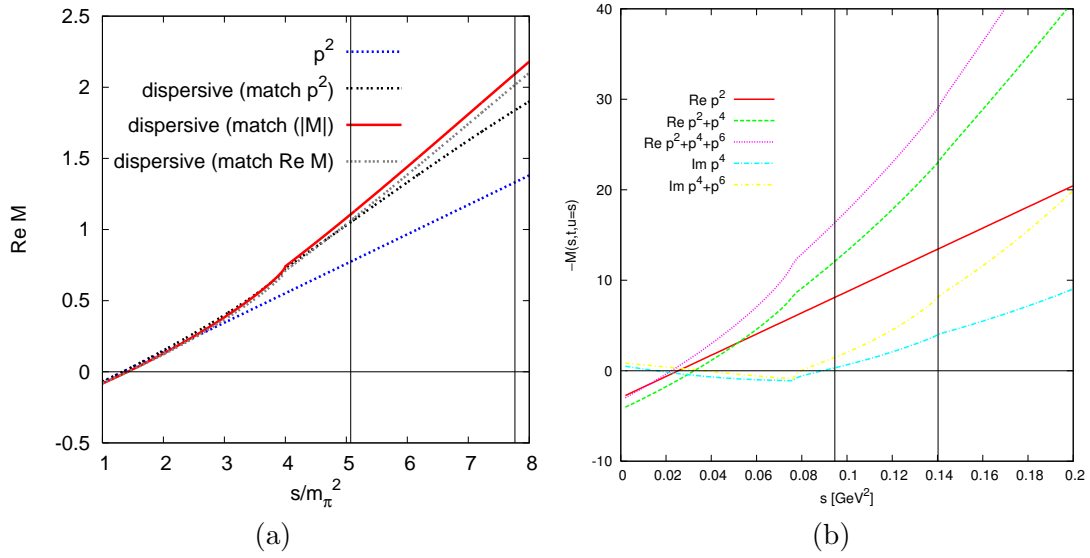


Figure 10: (a) The simplified analysis of [11] which shows the same general behaviour as the result of [20] shown in Fig. 9(b). (b) Our result for $M(s, t, u)$ at $s = u$.

In [20] the fact that the position of the Adler zero did not change much from LO to NLO was used to determine the subtraction constants. In Fig. 11 we show a blowup of the region around the Adler zero. As can be seen, the position of the zero in the real part varies a bit by going from LO to NLO and then almost moves back at NNLO. This is not incompatible with the observation of [20], we use a slightly different version of NLO than the one in [10] and use different input parameters resulting from the order p^6 determination of LECs [34].

The current algebra prediction for the Adler zero⁶ is $s = \frac{4}{3}m_\pi^2$, independent of t . The NLO effect produces a t dependent shift in the zero for the real part. A fairly large positive shift occurs along the line $t = u$ going from LO to NLO and a smaller negative shift from NLO to NNLO as can be seen in Fig. 7(a). Along the line $s = u$, a smaller positive shift appears from LO to NLO at $s = 1.70 m_\pi^2$ shifting to $s = 1.17 m_\pi^2$ at NNLO. The effects on the slopes can be judged from Figs. 7(a) and Fig. 11.

6.3 Dalitz Plot Parameters

In general we use the data averages of the particle data group (PDG)[13]. For the distributions in the Dalitz plot the PDG presents no averages. This distribution is usually

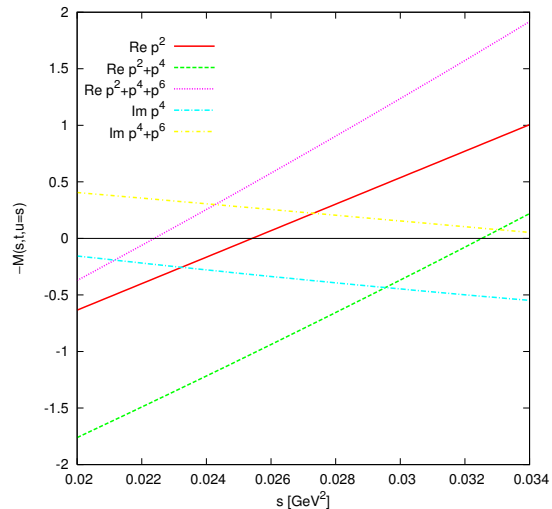


Figure 11: $M(s, t, u)$ along the line with $s = u$ concentrated along the Adler zero.

⁶We take here the zero of the real part of the amplitude as the Adler zero.

described in terms of the variables

$$\begin{aligned}
x &= \sqrt{3} \frac{T_+ - T_-}{Q_\eta} \\
y &= \frac{3T_0}{Q_\eta} - 1 \\
Q_\eta &= m_\eta - 2m_{\pi^+} - m_{\pi^0}
\end{aligned} \tag{6.1}$$

for the charged decay. T^i is the kinetic energy of pion π^i in the final state. The standard parameterization of the Dalitz plot is (up to third order)

$$|M|^2 = A_0^2 (1 + ay + by^2 + dx^2 + fy^3 + gx^2y + \dots) . \tag{6.2}$$

Odd terms in x are forbidden by charge conjugation, all experimental results find them compatible with zero and since all most precise experiments have presented fits with the odd terms set to zero we use those. f has only been measured by KLOE [50] and no experiment has attempted to determine g . Earlier experiments that only determined a and b are not included. The results are shown in Tab. 2. There are discrepancies among data

Exp.	a	b	d
KLOE [50]	$-1.090 \pm 0.005^{+0.008}_{-0.019}$	$0.124 \pm 0.006 \pm 0.010$	$0.057 \pm 0.006^{+0.007}_{-0.016}$
Crystal Barrel [51]	-1.22 ± 0.07	0.22 ± 0.11	0.06 ± 0.04 (input)
Layter et al. [52]	-1.08 ± 0.014	0.034 ± 0.027	0.046 ± 0.031
Gormley et al. [53]	-1.17 ± 0.02	0.21 ± 0.03	0.06 ± 0.04

Table 2: Measurements of the Dalitz plot distributions in $\eta \rightarrow \pi^+\pi^-\pi^0$. The parameters are defined in Eq. (6.2). The KLOE[50] for f is $f = 0.14 \pm 0.01 \pm 0.02$. None of the others determined f . The Crystal Barrel used d as input, but remarked that a and b varied very little within the range of d used.

which are hard for us to discuss since correlations are important. There is however a clear discrepancy between KLOE[50] and Gormley et al.[53] for a , KLOE[50], Gormley et al.[53] and Layter et al.[52] have three rather incompatible number for b . The results for d are all compatible.

Similarly the neutral decay is parameterized by

$$|\overline{M}|^2 = \overline{A}_0^2 (1 + 2\alpha z + \dots) . \quad z = \frac{2}{3} \sum_{i=1,3} \left(\frac{3E_i - m_\eta}{m_\eta - 3m_\pi^0} \right)^2 . \tag{6.3}$$

E_i is the energy of the i th pion in the final state. The parameter α has been measured by several experiments. There are two recent high precision measurements but they are in disagreement, however, KLOE published a new analysis very recently.

Let us now discuss how to extract the Dalitz parameters in chiral perturbation theory. First for the charged decay. The Dalitz plot variables x and y are related to the kinetic energy of the outgoing particles. In terms of Mandelstam parameters they are given as,

$$x = \frac{\sqrt{3}}{2m_\eta Q_\eta} (u - t)$$

$$y = \frac{3}{2m_\eta Q_\eta} ((m_\eta - m_{\pi^0})^2 - s) - 1 \stackrel{\text{iso}}{=} \frac{3}{2m_\eta Q_\eta} (s_0 - s) . \quad (6.4)$$

The first equality is valid in general, the second only in the isospin limit. Our amplitudes are in the isospin limit, with a common pion mass everywhere. The physical value gives $Q_\eta = m_\eta - 2m_{\pi^+} - m_{\pi^0} = 0.13318$. For the pion mass we used, $3m_\pi^2 = 2m_{\pi^+}^2 + m_{\pi^0}^2$, we get $Q_\eta = 0.13313$ MeV. So the value of Q_η is fine. In the isospin limit, $x = y = 0$ and $s = t = u = s_0$ coincide. In the physical case there is a small difference, $s = t = u = s_0$ corresponds to $y = -0.052$.

We evaluate the decay amplitude $M(s, t, u)$ in the s - t plane over the physical region. Since only two variables s and t are independent the relation $s + t + u = m_\eta^2 + 2m_{\pi^+}^2 + m_{\pi^0}^2$ is used to eliminate the third Mandelstam variable u in the amplitude. We then fit (6.2) to the amplitude $|M|^2 = |M^{(2)} + M^{(4)} + M^{(6)}|^2$ with as error $\Delta = \text{Re}M^{(6)}\text{Re}(M^{(2)} + M^{(4)} + M^{(6)}) + \text{Im}M^{(6)}\text{Im}(M^{(2)} + M^{(4)} + M^{(6)})$.

Exp.	α
KLOE [54]	$-0.027 \pm 0.004^{+0.004}_{-0.006}$
KLOE (prel)[55]	$-0.014 \pm 0.005 \pm 0.004$
Crystal Ball [56]	-0.031 ± 0.004
WASA/CELSIUS [57]	$-0.026 \pm 0.010 \pm 0.010$
Crystal Barrel [58]	$-0.052 \pm 0.017 \pm 0.010$
GAMS2000 [59]	-0.022 ± 0.023
SND [60]	$-0.010 \pm 0.021 \pm 0.010$

Table 3: Measurements of the Dalitz plot distribution in $\eta \rightarrow \pi^0 \pi^0 \pi^0$. The parameter α is defined in Eq. (6.3).

This is half of the NNLO contribution. The fitting error quoted in the result (6.5) is from this error, not from errors in the input values of the C_i^r and other LECs. For y we used the second expression in (6.4). The fits have been performed to $|M^{(2)}|^2$, $|M^{(2)} + M^{(4)}|^2$ and $|M^{(2)} + M^{(4)} + M^{(6)}|^2$ labeled LO, NLO and NNLO respectively. In NNLO we have studied the effect of setting the $C_i^r = 0$ and setting $L_i^r = C_i^r = 0$ and in NLO for $L_i^r = 0$. In addition, we have checked how much changing y from the second to the first expression in (6.4) changes the results, labeled NNLOp as well as including the g term and the terms with x^4, x^2y^2, y^4 , labeled NNLOq. The results are given in Tab. 4. The changes in going from NLO to NNLO are rather modest, the main change is the overall normalization A_0^2 . The linear slope a is lowered somewhat but not enough to reach the most recent experimental value. The same comment applies to the quadratic slope b . d is in agreement with the experimental values. f is always much smaller than the measured value of KLOE. The results from the dispersive calculations using Khuri-Treiman[19]⁷ and the simplified analysis of [11] with two different boundary conditions are also shown in the table. [21] used these parameters as input and we have therefore not shown their result. As final result we take the NNLO result of Tab. 4 with the MINUIT errors with inputs as above.

$$\begin{aligned} A_0^2 &= 538 \pm 18, \\ a &= -1.271 \pm 0.075, \\ b &= 0.394 \pm 0.102, \end{aligned}$$

⁷Note that there exists an analysis [61] using the method of [19] fitting the preliminary KLOE results. However, their final normalization depends on the allowed ranges of parameters given by [19]. This is why we do not quote their numbers below.

	A_0^2	a	b	d	f
LO	120	-1.039	0.270	0.000	0.000
NLO	314	-1.371	0.452	0.053	0.027
NNLO ($L_i^r = 0$)	235	-1.263	0.407	0.050	0.015
NNLO	538	-1.271	0.394	0.055	0.025
NNLOp	574	-1.229	0.366	0.052	0.023
NNLOq	535	-1.257	0.397	0.076	0.004
NNLO ($\mu = 0.6$ GeV)	543	-1.300	0.415	0.055	0.024
NNLO ($\mu = 0.9$ GeV)	548	-1.241	0.374	0.054	0.025
NNLO ($C_i^r = 0$)	465	-1.297	0.404	0.058	0.032
NNLO ($L_i^r = C_i^r = 0$)	251	-1.241	0.424	0.050	0.007
dispersive[19]	—	-1.33	0.26	0.10	—
tree dispersive[11]	—	-1.10	0.33	0.001	—
absolute dispersive[11]	—	-1.21	0.33	0.04	—

Table 4: Theoretical estimate of the Dalitz plot distributions in $\eta \rightarrow \pi^+ \pi^- \pi^0$. The parameters are defined in Eq. (6.2). The line labeled NNLO is our central result.

$$\begin{aligned}
d &= 0.055 \pm 0.057, \\
f &= 0.025 \pm 0.160.
\end{aligned}
\tag{6.5}$$

The fitting results for the neutral decay are shown in Tab. 5. Again we have fitted LO, NLO, NNLO and removed the contributions from C_i^r and L_i^r to see their effects. The one labeled NNLOq is the same fit as NNLO but with the next two terms in the expansion around $s = t = u = s_0$ included in the fit. As in the case of the charged decay, one sees that going from NLO to NNLO does not seem to change much in the Dalitz plot distributions but changes mainly the overall normalization. It should be mentioned that because of the three terms in (3.20) large cancellations happen in the amplitude for $\eta \rightarrow 3\pi^0$. This, as well as an inequality between the slope parameters is derived in App. A. The inequality is always satisfied by our results and the equality which results under additional assumptions is reasonably well satisfied. Assuming the error on the NNLO result to be one half the NNLO contribution as we did for the charged case leads to

$$\begin{aligned}
\overline{A}_0^2 &= 4790 \pm 160 \\
\alpha &= 0.013 \pm 0.032.
\end{aligned}
\tag{6.6}$$

The results from the dispersive calculations using Khuri-Treiman[19] and the simplified analysis of [11] with two different boundary conditions are also shown in the table. No theoretical prediction comes near the experimental results of KLOE[54] and Crystal Ball[56] except for the result⁸ of [21].

⁸That reference combines a Chiral Lagrangian including the η' and a model for unitary resummations. Their good agreement with data is remarkable but should also be understood using more controlled approximations.

	\overline{A}_0^2	α
LO	1090	0.000
NLO	2810	0.013
NLO ($L_i^r = 0$)	2100	0.016
NNLO	4790	0.013
NNLOq	4790	0.014
NNLO ($C_i^r = 0$)	4140	0.011
NNLO ($L_i^r = C_i^r = 0$)	2220	0.016
dispersive[19]	—	— (0.007—0.014)
tree dispersive[11]	—	—0.0065
absolute dispersive[11]	—	—0.007
[21]	—	—0.031

Table 5: Theoretical estimates of the Dalitz plot distribution in $\eta \rightarrow \pi^0 \pi^0 \pi^0$. The parameter α is defined in Eq. (6.3). The line labeled NNLO is the main result.

It is clear from these results that further study on possible variations of input parameters of ChPT is needed. One puzzling observation is however that the main effect in the dispersive calculations is S -wave rescattering and the input parameters used here give a very good prediction for the scattering length a_0^0 [62].

6.4 The ratio r and decay rates

We can now proceed to calculate the various decay rates from our amplitude. Since the evaluation of the NNLO terms is very slow we have used the following procedure. The actual shape of the allowed s, t, u region in the physical charged decay is somewhat different from the one allowed with an equal pion mass. We therefore perform the integration over the physically allowed values of s, t, u for the neutral and charged case.

The matrix-element $|M|^2$ is dealt with similar to the previous subsection. First we fit $|M|^2$ with an expansion in x and y up to fourth order in x and y for the charged and neutral case. The values for x and y are calculated using the values for s, t, u with the formulas of the isospin limit with the pion mass as defined above.

Doing that leads to the decay widths for the decays where we have indicated the various orders

$$\begin{aligned}
\Gamma(\eta \rightarrow \pi^+ \pi^- \pi^0) &= \sin^2 \epsilon \cdot 0.572 \text{ MeV} && \text{LO}, \\
&\sin^2 \epsilon \cdot 1.59 \text{ MeV} && \text{NLO}, \\
&\sin^2 \epsilon \cdot 2.68 \text{ MeV} && \text{NNLO}, \\
&\sin^2 \epsilon \cdot 2.33 \text{ MeV} && \text{NNLO } C_i^r = 0, \\
\Gamma(\eta \rightarrow \pi^0 \pi^0 \pi^0) &= \sin^2 \epsilon \cdot 0.884 \text{ MeV} && \text{LO}, \\
&\sin^2 \epsilon \cdot 2.31 \text{ MeV} && \text{NLO}, \\
&\sin^2 \epsilon \cdot 3.94 \text{ MeV} && \text{NNLO}, \\
&\sin^2 \epsilon \cdot 3.40 \text{ MeV} && \text{NNLO } C_i^r = 0.
\end{aligned} \tag{6.7}$$

The numbers in (6.7) can be used to calculate the ratio of decay rates

$$r \equiv \frac{\Gamma(\eta \rightarrow \pi^0 \pi^0 \pi^0)}{\Gamma(\eta \rightarrow \pi^+ \pi^- \pi^0)}. \quad (6.8)$$

To lowest order and neglecting the differences in phase space this ratio is expected to be exactly 1.5. The correct treatment of phasespace and the slightly different pion mass used lead to

$$r_{\text{LO}} = 1.54. \quad (6.9)$$

At higher orders a significant change is found with

$$\begin{aligned} r_{\text{NLO}} &= 1.46. \\ r_{\text{NNLO}} &= 1.47. \\ r_{\text{NNLO } C_i^T=0} &= 1.46. \end{aligned} \quad (6.10)$$

The small changes from NLO to NNLO is because the higher order corrections mainly change the overall size of the amplitude, not its shape.

This should be compared with the experimental result[13] of

$$\begin{aligned} r &= 1.49 \pm 0.06 \quad \text{our average.} \\ r &= 1.43 \pm 0.04 \quad \text{our fit,} \end{aligned} \quad (6.11)$$

The different results are from the direct measurements or from the global fit to eta decays. Our results agree excellently with each value.

6.5 Discussion and the values of R and Q

One of the prime reasons to study the hadronic eta decay to pions is the direct determination of the double quark mass ratio, Q^2 defined as[39]

$$Q^2 = \frac{m_s^2 - \hat{m}^2}{m_d^2 - m_u^2} \quad (6.12)$$

The reason for considering this quantity is that is to first order independent of shift in the quark masses of the form

$$\begin{aligned} m_u &\rightarrow m_u + \alpha m_d m_s, \\ m_d &\rightarrow m_d + \alpha m_s m_u, \\ m_s &\rightarrow m_s + \alpha m_u m_d. \end{aligned} \quad (6.13)$$

Within the framework of standard ChPT such a change is unobservable, it can always be compensated by a change in the values of the LECs up to order p^8 effects. This was observed to order p^4 in [63] but the generalization to higher orders is obviously true. In our case, we are implicitly using assumptions on the values of the constants such that this shift is fixed as discussed in [34]. That is one of the reasons we pulled out an overall factor

of $\sin(\epsilon)$ rather than Q^{-2} out of the eta decay amplitude. To first order in isospin breaking we have

$$\sin(\epsilon) = \epsilon = \frac{\sqrt{3}}{4} \frac{m_d - m_u}{m_s - \hat{m}} = \frac{\sqrt{3}}{4} \frac{1}{R}, \quad (6.14)$$

where the last equality defines the ratio R .

Since the process is $\eta \rightarrow 3\pi$ is strongly protected from the electromagnetic interactions due to the chiral symmetry, we expect to obtain the value $m_d - m_u$ rather well from this process. So let us see what our results imply. Using the experimental value[13]

$$\Gamma(\eta \rightarrow \pi^+ \pi^- \pi^0) = 295 \pm 17 \text{ eV} \quad (6.15)$$

and (6.7) and (6.14) we obtain the values for R quoted in Tab. 6) in the line labeled $R(\eta)$. For comparison we also quote the values obtained at LO using

	LO	NLO	NNLO	NNLO ($C_i^r = 0$)
$R(\eta)$	19.1	31.8	42.2	38.7
R (Dashen)	44	44	37	—
R (Dashen-violation)	36	37	32	—
$Q(\eta)$	15.6	20.1	23.2	22.2
Q (Dashen)	24	24	22	—
Q (Dashen-violation)	22	22	20	—

Table 6: The isospin breaking quantities R are evaluated at p^2 , p^4 and p^6 . The Q values are given with $Q^2 \approx 12.7 R$. See text for details.

$$R = \frac{m_{K^0}^2 + m_{K^+}^2 - 2m_{\pi^0}^2}{2(m_{K^0}^2 - m_{K^+}^2)} \quad (6.16)$$

where the QCD part of the masses should be included only. The electromagnetic part of the K^0 and π^0 mass is taken to be negligible and we use

$$m_{K^+ \text{em}}^2 = x_D (m_{\pi^+}^2 - m_{\pi^0}^2). \quad (6.17)$$

We take $x_D = 1$ in the line labeled Dashen[12] and use the estimate $x_D = 1.84$ [64] for the line labeled Dashen-violation. The columns labeled NLO and NNLO quote the results from [34] using the same input. These used $m_s/\hat{m} = 24$ as input but changing it to 26 changes⁹ the value of R by about half a unit. Note that the limit $R < 44$ [39] is satisfied by all the estimates in Tab. 6.

It is harder to draw conclusions on the value of Q . Its value can be obtained from

$$Q^2 = \frac{m_K^2}{m_\pi^2} (1 + \text{NNLO}), \quad (6.18)$$

where again only the QCD part of the masses should be included and m_K^2, m_π^2 are the masses in the isospin limit. The NNLO corrections are known [34] and not negligible.

⁹This can be seen from using the number for m_u/m_d and m_s/\hat{m} from Fig. 3(b) in [34].

However, they do depend at present on the input value of m_s/\hat{m} used in the chiral fits, this can be seen in Fig. 3(a) of [34]. Varying m_s/\hat{m} from 24 to 26 changes Q by about one unit. The analysis of [39] relied on the NNLO correction being small.

The relation between Q^2 and R can be written as

$$Q^2 = \frac{1}{2} \left(1 + \frac{m_s}{\hat{m}} \right) R. \quad (6.19)$$

The analysis of [39] leads to a factor of about 12.7 using $m_s/\hat{m} = 24.4$, the input value for $m_s/\hat{m} = 24$ to about 12.5 and for $m_s/\hat{m} = 26$ to 13.5. After taking the square root, this range corresponds to an uncertainty on Q of about unit. For completeness we have listed in Tab. 6 the values of Q derived from R with the factor equal to 12.7.

7. Conclusions

In this paper we have performed a NNLO calculation in standard ChPT of the amplitude for $\eta \rightarrow 3\pi$. This calculation was performed to first order in isospin breaking and we have pulled out the overall factor in the form of $\sin(\epsilon)$, the lowest order π^0 - η mixing angle. The remainder of the amplitude is then dealt with in the isospin limit. How we have dealt with the pion mass is described in Sect. 6.1 and with the Dalitz plot distributions and decay rates in Sects. 6.3 and 6.4.

We find a reasonable enhancement over the NLO result of [10] which is somewhat larger than the estimates from the dispersive analyses [19, 20]. The shape of the amplitude is in better agreement with [20] from comparing the published plots along the line $s = u$. We have also commented on the position of the Adler zero which was used in [20] to determine their subtraction constants. The NNLO result for the Dalitz plot distributions moves somewhat in the direction of the experimental results compared to the NLO result but is not in good agreement. The same is also true for the slope parameter α in the neutral decay. We always obtain a positive value while experiment is consistently negative. The amplitude for this decay has large cancellations and that makes α a difficult parameter to predict, however all methods which include unitarity resummations and have published values [11, 19, 21] get a negative value. This we find puzzling, since the main effect is $\pi\pi$ S -wave rescattering and our input values give a good value for the scattering length a_0^0 [62]. We obtain very good agreement with the ratio r .

Since we find a somewhat larger enhancement of the decay rate than [20] we also find a somewhat larger value for the isospin breaking quantities R and Q , which means that $m_d - m_u$ is somewhat smaller than obtained in [39]. We also find values that are not in agreement with the NNLO order fit to the meson masses [34].

The influence of changes in the input values is under study, a first impression can be had from looking at the results for the $C_i^r = 0$ and the different choices of μ . A more detailed analysis is planned.

Acknowledgments

This work is supported in part by the European Commission RTN network, Contract MRTN-CT-2006-035482 (FLAVIANet), the European Community-Research Infrastructure

Activity Contract RII3-CT-2004-506078 (HadronPhysics) and the Swedish Research Council.

A. A discussion on Dalitzplotparameters and the sign of α

The goal of this appendix is to point a few simple observations about relations between the Dalitzplot parameters. We start by parameterizing the amplitude for the charged decay rate as

$$\begin{aligned} M(s, t, u) &= A \left(1 + \tilde{a}(s - s_0) + \tilde{b}(s - s_0)^2 + \tilde{d}(u - t)^2 + \dots \right) \\ &= A \left(1 + \bar{a}y + \bar{b}y^2 + \bar{d}x^2 + \dots \right) \end{aligned} \quad (\text{A.1})$$

By computing $|M(s, t, u)|^2$ and using (6.4) this leads to the relations

$$\begin{aligned} a &= 2 \operatorname{Re}(\bar{a}) = -2R_\eta \operatorname{Re}(\tilde{a}), \\ b &= |\bar{a}|^2 + 2\operatorname{Re}(\bar{b}) = R_\eta^2 \left(|\tilde{a}|^2 + 2\operatorname{Re}(\tilde{b}) \right), \\ d &= 2\operatorname{Re}(\bar{d}) = 6R_\eta^2 \operatorname{Re}(\tilde{d}). \end{aligned} \quad (\text{A.2})$$

Here we defined $R_\eta = (2m_\eta Q_\eta)/3$. We can now use relation (3.20) and $s + t + u = 3s_0$ we obtain

$$\begin{aligned} \bar{M}(s, t, u) &\equiv \bar{A} (1 + \bar{\alpha}z + \dots) \\ &= A \left(3 + (\tilde{b} + 3\tilde{d}) \left((s - s_0)^2 + (t - s_0)^2 + (u - s_0)^2 \right) + \dots \right) \end{aligned} \quad (\text{A.3})$$

Using the definition of z these two can be related and give

$$\bar{A} = 3A, \quad (\text{A.4})$$

as well

$$\alpha = \operatorname{Re}(\bar{\alpha}) = \frac{1}{2} R_\eta^2 \operatorname{Re}(\tilde{b} + 3\tilde{d}) = \frac{1}{4} (d + b - R_\eta^2 |\tilde{a}|^2). \quad (\text{A.5})$$

We thus obtain the relation

$$\alpha \geq \frac{1}{4} \left(d + b - \frac{1}{4} a^2 \right). \quad (\text{A.6})$$

Under the *assumption* that $\operatorname{Im}(\tilde{a}) = 0$, this turns into an equality. If one looks at the numbers in Tabs. 2 and 4 we see that there is a very strong cancellation on the r.h.s. of (A.6). Note that the KLOE results satisfy the relation with equality quite well and the theory results satisfy it within 30% or so. The inequality is satisfied in all cases. The underlying reason why it is difficult to get a negative α seems to be that the value obtained for b is too large compared to experiment.

For our NNLO result we can perform the fit also to the amplitude directly and we obtain

$$\begin{aligned} A &= -22.7 - i 4.38, \\ \bar{a} &= -0.631 - i 0.183, \\ \bar{b} &= -0.017 + i 0.025, \\ \bar{d} &= 0.040 - i 0.023. \end{aligned} \quad (\text{A.7})$$

We see that the relation (A.2) is satisfied. In general, \bar{a} is sizable but \bar{b} , \bar{c} , and the higher order in x, y generalizations are small.

B. The order p^4 expression

In this appendix we quote the precise way in which we have defined the order p^4 contribution. It agrees with the result of [10]. We use the notation

$$P_{\eta\pi} = m_\eta^2 - m_{\pi^0}^2. \quad (\text{B.1})$$

This appears after Δm_1^2 and Δm_2^2 of (3.11) have been rewritten in the physical masses.

The functions are defined in (4.2).

$$\begin{aligned} M_0^{(4)}(s) = & +L_8^r \left(32 m_{K^0}^2 s - 32 m_{\pi^0}^2 s - 256/3 m_{\pi^0}^2 m_{K^0}^2 + 256/3 m_{\pi^0}^4 \right) \\ & +L_7^r \left(96 m_{K^0}^2 s - 96 m_{\pi^0}^2 s - 640/3 m_{\pi^0}^2 m_{K^0}^2 + 640/3 m_{\pi^0}^4 \right) \\ & +L_5^r \left(-8 m_{\pi^0}^2 s + 64/9 m_{\pi^0}^2 m_{K^0}^2 + 32/9 m_{\pi^0}^4 \right) \\ & +L_3^r \left(-16/9 s^2 + 16/3 m_{K^0}^2 s - 64/27 m_{K^0}^4 + 32/3 m_{\pi^0}^2 s - 256/27 m_{\pi^0}^2 m_{K^0}^2 - 256/27 m_{\pi^0}^4 \right) \\ & +\frac{1}{16\pi^2} \left(1/9 s^2 + 1/6 m_{K^0}^2 s - 2/27 m_{K^0}^4 + 1/3 m_{\pi^0}^2 s - 8/27 m_{\pi^0}^2 m_{K^0}^2 - 8/27 m_{\pi^0}^4 \right) \\ & +\bar{A}(m_{\pi^0}^2) P_{\eta\pi}^{-1} \left(4/3 m_{\pi^0}^2 s - 16/9 m_{\pi^0}^4 \right) + \bar{A}(m_{\pi^0}^2) \left(-3/2 s + 4/9 m_{K^0}^2 + 20/9 m_{\pi^0}^2 \right) \\ & +\bar{A}(m_{K^0}^2) P_{\eta\pi}^{-1} \left(-4/3 m_{\pi^0}^2 s + 16/9 m_{\pi^0}^4 \right) + \bar{A}(m_{K^0}^2) \left(-1/2 s + 2/9 m_{K^0}^2 - 2/9 m_{\pi^0}^2 \right) \\ & +\bar{A}(m_\eta^2) \left(1/2 s - 2/3 m_{\pi^0}^2 \right) \\ & +\bar{B}(m_{\pi^0}^2, m_{\pi^0}^2, s) \left(-2/3 s^2 - 4/9 m_{K^0}^2 s + 5/3 m_{\pi^0}^2 s + 2/9 m_{\pi^0}^2 m_{K^0}^2 - 2/3 m_{\pi^0}^4 \right) \\ & +\bar{B}(m_{\pi^0}^2, m_\eta^2, s) \left(-2/9 m_{\pi^0}^2 s - 4/27 m_{\pi^0}^2 m_{K^0}^2 + 4/9 m_{\pi^0}^4 \right) \\ & +\bar{B}(m_{K^0}^2, m_{K^0}^2, s) \left(1/2 s^2 - 2/3 m_{K^0}^2 s + 4/9 m_{K^0}^4 - 1/3 m_{\pi^0}^2 s \right) \\ & +\bar{B}(m_{K^0}^2, m_{K^0}^2, 0) \left(3/2 m_{K^0}^2 s - 2/3 m_{K^0}^4 - 1/2 m_{\pi^0}^2 s - 2/3 m_{\pi^0}^2 m_{K^0}^2 \right) \\ & +\bar{B}(m_\eta^2, m_\eta^2, s) \left(2/9 m_{\pi^0}^2 m_{K^0}^2 - 2/9 m_{\pi^0}^4 \right) \\ & +\bar{C}(m_{K^0}^2, m_{K^0}^2, m_{K^0}^2, s) \left(-1/2 m_{K^0}^2 s^2 + 2/3 m_{K^0}^4 s + 1/2 m_{\pi^0}^2 s^2 - 2/3 m_{\pi^0}^2 m_{K^0}^2 \right) \end{aligned} \quad (\text{B.2})$$

$$M_1^{(4)}(t) = \bar{B}(m_{\pi^0}^2, m_{\pi^0}^2, t) \left(-1/12 t + 1/3 m_{\pi^0}^2 \right) + \bar{B}(m_{K^0}^2, m_{K^0}^2, t) \left(-1/24 t + 1/6 m_{K^0}^2 \right). \quad (\text{B.3})$$

$$\begin{aligned}
M_2^{(4)}(t) = & L_3^r \left(4/3 t^2 \right) + \frac{1}{16\pi^2} \left(-1/12 t^2 \right) \\
& + \overline{B}(m_{\pi^0}^2, m_{\pi^0}^2, t) \left(-1/4 t^2 + 1/3 m_{K^0}^2 t + 1/2 m_{\pi^0}^2 t - 2/3 m_{\pi^0}^2 m_{K^0}^2 \right) \\
& + \overline{B}(m_{\pi^0}^2, m_{\eta}^2, t) \left(1/6 m_{\pi^0}^2 t - 2/9 m_{\pi^0}^2 m_{K^0}^2 \right) + \overline{B}(m_{K^0}^2, m_{K^0}^2, t) \left(3/8 t^2 - m_{K^0}^2 t + 2/3 m_{K^0}^4 \right).
\end{aligned} \tag{B.4}$$

C. The order p^6 LECs dependent part

In this appendix we give the amplitude dependence on the order p^6 LECs C_i^r in the form of $M_I^C(t)$ as defined (4.4).

$$\begin{aligned}
M_0^C(s) = & +C_{33}^r \left(256 m_{K^0}^4 s - 512/9 m_{K^0}^6 - 128 m_{\pi^0}^2 m_{K^0}^2 s - 1280/9 m_{\pi^0}^2 m_{K^0}^4 - 128 m_{\pi^0}^4 s \right. \\
& \left. - 5120/9 m_{\pi^0}^4 m_{K^0}^2 + 768 m_{\pi^0}^6 \right) \\
& +C_{32}^r \left(128 m_{K^0}^4 s - 512/9 m_{K^0}^6 - 64 m_{\pi^0}^2 m_{K^0}^2 s - 1280/9 m_{\pi^0}^2 m_{K^0}^4 \right. \\
& \left. - 64 m_{\pi^0}^4 s - 1280/9 m_{\pi^0}^4 m_{K^0}^2 + 1024/3 m_{\pi^0}^6 \right) \\
& +C_{31}^r \left(128 m_{K^0}^4 s - 512/9 m_{K^0}^6 - 64 m_{\pi^0}^2 m_{K^0}^2 s - 256/3 m_{\pi^0}^2 m_{K^0}^4 \right. \\
& \left. - 64 m_{\pi^0}^4 s - 1024/3 m_{\pi^0}^4 m_{K^0}^2 + 4352/9 m_{\pi^0}^6 \right) \\
& +C_{29}^r \left(128/3 m_{\pi^0}^2 m_{K^0}^2 s + 64/3 m_{\pi^0}^4 s - 256/9 m_{\pi^0}^4 m_{K^0}^2 - 512/9 m_{\pi^0}^6 \right) \\
& +C_{28}^r \left(256/3 m_{K^0}^4 s - 512/3 m_{\pi^0}^2 m_{K^0}^2 s - 512/3 m_{\pi^0}^2 m_{K^0}^4 + 256/3 m_{\pi^0}^4 s \right. \\
& \left. + 1024/3 m_{\pi^0}^4 m_{K^0}^2 - 512/3 m_{\pi^0}^6 \right) \\
& +C_{27}^r \left(128/3 m_{K^0}^4 s - 256/3 m_{\pi^0}^2 m_{K^0}^2 s - 512/9 m_{\pi^0}^2 m_{K^0}^4 + 128/3 m_{\pi^0}^4 s \right. \\
& \left. + 1792/9 m_{\pi^0}^4 m_{K^0}^2 - 1280/9 m_{\pi^0}^6 \right) \\
& +C_{26}^r \left(-64/3 m_{\pi^0}^2 m_{K^0}^2 s + 256/9 m_{\pi^0}^2 m_{K^0}^4 - 32/3 m_{\pi^0}^4 s + 128/3 m_{\pi^0}^4 m_{K^0}^2 - 256/9 m_{\pi^0}^6 \right) \\
& +C_{25}^r \left(-32/3 m_{K^0}^2 s^2 + 64/9 m_{K^0}^4 s - 32/9 m_{\pi^0}^2 s^2 + 256/9 m_{\pi^0}^2 m_{K^0}^2 s - 256/27 m_{\pi^0}^2 m_{K^0}^4 \right. \\
& \left. + 256/9 m_{\pi^0}^4 s - 1024/27 m_{\pi^0}^4 m_{K^0}^2 - 1024/27 m_{\pi^0}^6 \right) \\
& +C_{24}^r \left(-160/9 m_{K^0}^2 s^2 - 64/3 m_{K^0}^4 s + 512/27 m_{K^0}^6 + 160/9 m_{\pi^0}^2 s^2 \right. \\
& \left. + 128/3 m_{\pi^0}^2 m_{K^0}^2 s + 256/9 m_{\pi^0}^2 m_{K^0}^4 - 64/3 m_{\pi^0}^4 s - 256/9 m_{\pi^0}^4 m_{K^0}^2 - 512/27 m_{\pi^0}^6 \right) \\
& +C_{22}^r \left(-64/9 m_{K^0}^2 s^2 - 256/9 m_{K^0}^4 s + 512/27 m_{K^0}^6 + 64/3 m_{\pi^0}^2 s^2 \right. \\
& \left. + 128/9 m_{\pi^0}^2 m_{K^0}^2 s + 1024/27 m_{\pi^0}^2 m_{K^0}^4 - 448/9 m_{\pi^0}^4 s + 256/27 m_{\pi^0}^4 m_{K^0}^2 + 512/27 m_{\pi^0}^6 \right) \\
& +C_{21}^r \left(-256/3 m_{K^0}^6 + 64 m_{\pi^0}^4 m_{K^0}^2 + 64/3 m_{\pi^0}^6 \right)
\end{aligned}$$

$$\begin{aligned}
& +C_{20}^r \left(128 m_{K^0}^4 s - 256/3 m_{K^0}^6 - 64 m_{\pi^0}^2 m_{K^0}^2 s - 256/3 m_{\pi^0}^2 m_{K^0}^4 - 64 m_{\pi^0}^4 s \right. \\
& \left. - 192 m_{\pi^0}^4 m_{K^0}^2 + 1088/3 m_{\pi^0}^6 \right) \\
& +C_{19}^r \left(192 m_{K^0}^4 s - 256/3 m_{K^0}^6 - 96 m_{\pi^0}^2 m_{K^0}^2 s - 128 m_{\pi^0}^2 m_{K^0}^4 - 96 m_{\pi^0}^4 s \right. \\
& \left. - 320 m_{\pi^0}^4 m_{K^0}^2 + 1600/3 m_{\pi^0}^6 \right) \\
& +C_{18}^r \left(- 320/3 m_{K^0}^4 s + 512/27 m_{K^0}^6 + 352/3 m_{\pi^0}^2 m_{K^0}^2 s + 256/3 m_{\pi^0}^2 m_{K^0}^4 - 32/3 m_{\pi^0}^4 s \right. \\
& \left. - 128/9 m_{\pi^0}^4 m_{K^0}^2 - 2432/27 m_{\pi^0}^6 \right) \\
& +C_{17}^r \left(- 64/3 m_{K^0}^4 s + 512/27 m_{K^0}^6 + 32 m_{\pi^0}^2 m_{K^0}^2 s - 256/27 m_{\pi^0}^2 m_{K^0}^4 - 80/3 m_{\pi^0}^4 s \right. \\
& \left. + 1472/27 m_{\pi^0}^4 m_{K^0}^2 - 128/3 m_{\pi^0}^6 \right) \\
& +C_{16}^r \left(448/3 m_{K^0}^4 s + 256/9 m_{K^0}^6 - 704/3 m_{\pi^0}^2 m_{K^0}^2 s - 2816/9 m_{\pi^0}^2 m_{K^0}^4 + 400/3 m_{\pi^0}^4 s \right. \\
& \left. + 4288/9 m_{\pi^0}^4 m_{K^0}^2 - 256 m_{\pi^0}^6 \right) \\
& +C_{15}^r \left(512/27 m_{K^0}^6 + 256/9 m_{\pi^0}^2 m_{K^0}^4 - 256/9 m_{\pi^0}^4 m_{K^0}^2 - 512/27 m_{\pi^0}^6 \right) \\
& +C_{14}^r \left(- 64/3 m_{K^0}^4 s + 512/27 m_{K^0}^6 - 32 m_{\pi^0}^2 m_{K^0}^2 s + 512/27 m_{\pi^0}^2 m_{K^0}^4 + 112/3 m_{\pi^0}^4 s \right. \\
& \left. + 2240/27 m_{\pi^0}^4 m_{K^0}^2 - 896/9 m_{\pi^0}^6 \right) \\
& +C_{13}^r \left(- 128/3 m_{K^0}^2 s^2 + 128 m_{K^0}^4 s - 512/27 m_{K^0}^6 - 64/3 m_{\pi^0}^2 s^2 + 320 m_{\pi^0}^2 m_{K^0}^2 s \right. \\
& \left. - 1792/9 m_{\pi^0}^2 m_{K^0}^4 + 128 m_{\pi^0}^4 s - 3584/9 m_{\pi^0}^4 m_{K^0}^2 - 4096/27 m_{\pi^0}^6 \right) \\
& +C_{12}^r \left(64/9 m_{K^0}^2 s^2 + 512/9 m_{K^0}^4 s + 512/81 m_{K^0}^6 - 64/3 m_{\pi^0}^2 s^2 - 256/9 m_{\pi^0}^2 m_{K^0}^2 s \right. \\
& \left. - 1024/9 m_{\pi^0}^2 m_{K^0}^4 + 896/9 m_{\pi^0}^4 s + 1792/27 m_{\pi^0}^4 m_{K^0}^2 - 10496/81 m_{\pi^0}^6 \right) \\
& +C_{11}^r \left(128/9 m_{K^0}^2 s^2 - 128/3 m_{K^0}^4 s + 512/27 m_{K^0}^6 + 64/9 m_{\pi^0}^2 s^2 - 320/3 m_{\pi^0}^2 m_{K^0}^2 s \right. \\
& \left. + 256/3 m_{\pi^0}^2 m_{K^0}^4 - 128/3 m_{\pi^0}^4 s + 1024/9 m_{\pi^0}^4 m_{K^0}^2 + 1024/27 m_{\pi^0}^6 \right) \\
& +C_{10}^r \left(- 32/9 m_{K^0}^2 s^2 - 64/9 m_{K^0}^4 s + 256/27 m_{K^0}^6 + 32/3 m_{\pi^0}^2 s^2 - 256/9 m_{\pi^0}^2 m_{K^0}^2 s \right. \\
& \left. + 256/27 m_{\pi^0}^2 m_{K^0}^4 - 256/9 m_{\pi^0}^4 s + 1408/27 m_{\pi^0}^4 m_{K^0}^2 + 128/9 m_{\pi^0}^6 \right) \\
& +C_9^r \left(- 160/9 m_{K^0}^2 s^2 + 512/27 m_{K^0}^6 + 160/9 m_{\pi^0}^2 s^2 - 256/9 m_{\pi^0}^2 m_{K^0}^4 + 128/3 m_{\pi^0}^4 m_{K^0}^2 \right. \\
& \left. - 896/27 m_{\pi^0}^6 \right) \\
& +C_8^r \left(- 32/9 m_{K^0}^2 s^2 - 64/9 m_{K^0}^4 s + 256/27 m_{K^0}^6 + 32/9 m_{\pi^0}^2 m_{K^0}^2 s - 128/27 m_{\pi^0}^2 m_{K^0}^4 \right. \\
& \left. + 320/9 m_{\pi^0}^4 s - 128/27 m_{\pi^0}^4 m_{K^0}^2 - 128/3 m_{\pi^0}^6 \right) \\
& +C_6^r \left(- 64/9 m_{K^0}^2 s^2 + 64/3 m_{K^0}^4 s - 256/27 m_{K^0}^6 - 32/9 m_{\pi^0}^2 s^2 + 160/3 m_{\pi^0}^2 m_{K^0}^2 s \right. \\
& \left. - 128/3 m_{\pi^0}^2 m_{K^0}^4 + 64/3 m_{\pi^0}^4 s - 512/9 m_{\pi^0}^4 m_{K^0}^2 - 512/27 m_{\pi^0}^6 \right)
\end{aligned}$$

$$\begin{aligned}
& +C_5^r \left(-32/3 m_{K^0}^2 s^2 + 128/9 m_{K^0}^4 s + 64/9 m_{\pi^0}^2 s^2 + 224/9 m_{\pi^0}^2 m_{K^0}^2 s - 896/27 m_{\pi^0}^2 m_{K^0}^4 \right. \\
& \left. -64/9 m_{\pi^0}^4 s - 128/27 m_{\pi^0}^4 m_{K^0}^2 - 128/27 m_{\pi^0}^6 \right) \\
& +C_4^r \left(-64/9 s^3 + 128/27 m_{K^0}^2 s^2 + 128/9 m_{K^0}^4 s - 512/81 m_{K^0}^6 + 256/27 m_{\pi^0}^2 s^2 \right. \\
& \left. -256/9 m_{\pi^0}^2 m_{K^0}^2 s + 128/9 m_{\pi^0}^4 s + 512/27 m_{\pi^0}^4 m_{K^0}^2 - 1024/81 m_{\pi^0}^6 \right) \\
& +C_3^r \left(-64/9 s^3 + 128/9 m_{K^0}^2 s^2 - 128/9 m_{K^0}^4 s + 512/81 m_{K^0}^6 + 256/9 m_{\pi^0}^2 s^2 \right. \\
& \left. -896/9 m_{\pi^0}^2 m_{K^0}^2 s \right. \\
& \left. +512/9 m_{\pi^0}^2 m_{K^0}^4 - 704/9 m_{\pi^0}^4 s + 3328/27 m_{\pi^0}^4 m_{K^0}^2 + 5632/81 m_{\pi^0}^6 \right) \\
& +C_1^r \left(32/9 s^3 - 64/9 m_{K^0}^2 s^2 + 64/9 m_{K^0}^4 s - 256/81 m_{K^0}^6 - 128/9 m_{\pi^0}^2 s^2 \right. \\
& \left. +448/9 m_{\pi^0}^2 m_{K^0}^2 s - 256/9 m_{\pi^0}^2 m_{K^0}^4 + 352/9 m_{\pi^0}^4 s - 1664/27 m_{\pi^0}^4 m_{K^0}^2 - 2816/81 m_{\pi^0}^6 \right)
\end{aligned} \tag{C.1}$$

$$M_1^C(t) = 0. \tag{C.2}$$

$$\begin{aligned}
M_2^C(t) = & C_{25}^r \left(32/3 m_{\pi^0}^2 t^2 \right) + C_{24}^r \left(-32/3 m_{K^0}^2 t^2 + 32/3 m_{\pi^0}^2 t^2 \right) + C_{22}^r \left(-32/3 m_{K^0}^2 t^2 \right) \\
& +C_{13}^r \left(32 m_{K^0}^2 t^2 + 16 m_{\pi^0}^2 t^2 \right) + C_{12}^r \left(32/3 m_{K^0}^2 t^2 \right) \\
& +C_{11}^r \left(-32/3 m_{K^0}^2 t^2 - 16/3 m_{\pi^0}^2 t^2 \right) + C_{10}^r \left(-16/3 m_{K^0}^2 t^2 \right) \\
& +C_9^r \left(-32/3 m_{K^0}^2 t^2 + 32/3 m_{\pi^0}^2 t^2 \right) + C_8^r \left(-16/3 m_{K^0}^2 t^2 + 8 m_{\pi^0}^2 t^2 \right) \\
& +C_6^r \left(16/3 m_{K^0}^2 t^2 + 8/3 m_{\pi^0}^2 t^2 \right) + C_5^r \left(8/3 m_{\pi^0}^2 t^2 \right) \\
& +C_4^r \left(16/3 t^3 - 32/9 m_{K^0}^2 t^2 - 64/9 m_{\pi^0}^2 t^2 \right) + C_3^r \left(16/3 t^3 - 32/3 m_{K^0}^2 t^2 - 64/3 m_{\pi^0}^2 t^2 \right) \\
& +C_1^r \left(-8/3 t^3 + 16/3 m_{K^0}^2 t^2 + 32/3 m_{\pi^0}^2 t^2 \right)
\end{aligned} \tag{C.3}$$

References

- [1] J. Bijnens, G. Fäldt and B.M.K. Nefkens (eds.) Phys. Scripta **T99** (2002) 1-282
- [2] B. Höistad and P. Moskal (eds.), Acta Phys. Slov. **56** (2005) 193-409.
- [3] D. G. Sutherland Phys. Lett. **23** (1966) 384
- [4] J. S. Bell and D. G. Sutherland, Nucl. Phys. B **4** (1968) 315.
- [5] J. A. Cronin, Phys. Rev. **161** (1967) 1483.
- [6] H. Osborn and D. J. Wallace, Nucl. Phys. B **20** (1970) 23.
- [7] S. Weinberg, Physica A **96** (1979) 327.
- [8] J. Gasser and H. Leutwyler, Annals Phys. **158** (1984) 142.
- [9] J. Gasser and H. Leutwyler, Nucl. Phys. B **250** (1985) 465.

- [10] J. Gasser and H. Leutwyler, Nucl. Phys. B **250** (1985) 539.
- [11] J. Bijnens and J. Gasser, Phys. Scripta **T99** (2002) 34 [arXiv:hep-ph/0202242].
- [12] R. F. Dashen, Phys. Rev. **183** (1969) 1245.
- [13] W. M. Yao *et al.* [Particle Data Group], J. Phys. G **33** (2006) 1.
- [14] J. F. Donoghue, B. R. Holstein and D. Wyler, Phys. Rev. D **47** (1993) 2089.
- [15] J. Bijnens, Phys. Lett. B **306** (1993) 343 [arXiv:hep-ph/9302217].
- [16] R. Baur, J. Kambor and D. Wyler, Nucl. Phys. B **460** (1996) 127 [arXiv:hep-ph/9510396].
- [17] A. Neveu and J. Scherk, Annals Phys. **57** (1970) 39.
- [18] C. Roiesnel and T. N. Truong, Nucl. Phys. B **187** (1981) 293;
T. N. Truong, Nucl. Phys. Proc. Suppl. **24A** (1991) 93.
- [19] J. Kambor, C. Wiesendanger and D. Wyler, Nucl. Phys. B **465** (1996) 215
[arXiv:hep-ph/9509374].
- [20] A. V. Anisovich and H. Leutwyler, Phys. Lett. B **375** (1996) 335 [arXiv:hep-ph/9601237].
- [21] B. Borasoy and R. Nissler, Eur. Phys. J. A **26** (2005) 383 [arXiv:hep-ph/0510384].
- [22] S. Descotes-Genon, N. H. Fuchs, L. Girlanda and J. Stern, Eur. Phys. J. C **34** (2004) 201
[arXiv:hep-ph/0311120].
- [23] J. Bijnens, Prog. Part. Nucl. Phys. **58** (2007) 521 [arXiv:hep-ph/0604043].
- [24] J. Bijnens, G. Colangelo and J. Gasser, Nucl. Phys. B **427** (1994) 427
[arXiv:hep-ph/9403390].
- [25] G. Amorós, J. Bijnens and P. Talavera, Nucl. Phys. B **585** (2000) 293 [Erratum-ibid. B **598**
(2001) 665] [arXiv:hep-ph/0003258].
- [26] A. V. Manohar, arXiv:hep-ph/9606222.
- [27] V. Bernard, N. Kaiser and U. G. Meissner, Int. J. Mod. Phys. E **4** (1995) 193
[arXiv:hep-ph/9501384].
- [28] G. Ecker, Prog. Part. Nucl. Phys. **35** (1995) 1 [arXiv:hep-ph/9501357].
- [29] V. Bernard and U. G. Meissner, arXiv:hep-ph/0611231, to be published in Ann. Rev. Nucl.
Part. Sci.
- [30] J. Bijnens, G. Colangelo and G. Ecker, JHEP **9902** (1999) 020 [arXiv:hep-ph/9902437].
- [31] J. Bijnens, G. Colangelo, G. Ecker, J. Gasser and M. E. Sainio, Nucl. Phys. B **508** (1997) 263
[Erratum-ibid. B **517** (1998) 639] [arXiv:hep-ph/9707291].
- [32] J. Bijnens, G. Colangelo and G. Ecker, Annals Phys. **280** (2000) 100 [arXiv:hep-ph/9907333].
- [33] C. Aubin *et al.* [MILC Collaboration], Phys. Rev. D **70** (2004) 114501
[arXiv:hep-lat/0407028].
- [34] G. Amorós, J. Bijnens and P. Talavera, Nucl. Phys. B **602** (2001) 87 [arXiv:hep-ph/0101127].
- [35] G. Ecker, J. Gasser, A. Pich and E. de Rafael, Nucl. Phys. B **321** (1989) 311.
- [36] V. Cirigliano, G. Ecker, M. Eidemuller, R. Kaiser, A. Pich and J. Portoles, Nucl. Phys. B
753 (2006) 139 [arXiv:hep-ph/0603205].

- [37] G. Ecker, J. Gasser, H. Leutwyler, A. Pich and E. de Rafael, Phys. Lett. B **223** (1989) 425.
- [38] J. Bijnens, E. Gamiz, E. Lipartia and J. Prades, JHEP **0304** (2003) 055 [arXiv:hep-ph/0304222].
- [39] H. Leutwyler, Phys. Lett. B **378** (1996) 313 [arXiv:hep-ph/9602366].
- [40] M. Knecht, B. Moussallam, J. Stern and N. H. Fuchs, Nucl. Phys. B **457** (1995) 513 [arXiv:hep-ph/9507319].
- [41] J. Bijnens, P. Dhonte and F. Persson, Nucl. Phys. B **648** (2003) 317 [arXiv:hep-ph/0205341].
- [42] G. Amorós, J. Bijnens and P. Talavera, Nucl. Phys. B **568** (2000) 319 [arXiv:hep-ph/9907264].
- [43] J. Bijnens and P. Talavera, JHEP **0203**, 046 (2002) [arXiv:hep-ph/0203049].
- [44] S. Necco, talk at Lattice 2007
- [45] H. Leutwyler, Phys. Lett. B **374** (1996) 181 [arXiv:hep-ph/9601236].
- [46] R. Kaiser and H. Leutwyler, Eur. Phys. J. C **17** (2000) 623 [arXiv:hep-ph/0007101].
- [47] R. Kaiser, talk presented at EuroFlavour06, 2-4 November 2006, Barcelona, Spain.
- [48] K. Kampf, J. Novotny and J. Trnka, Eur. Phys. J. C **50** (2007) 385 [arXiv:hep-ph/0608051].
- [49] J. Bijnens, Acta Phys. Slov. **56** (2005) 305 [arXiv:hep-ph/0511076].
- [50] F. Ambrosino *et al.* [KLOE Collaboration], arXiv:0707.2355 [hep-ex].
- [51] A. Abele *et al.* [Crystal Barrel Collaboration], Phys. Lett. B **417** (1998) 197.
- [52] J. G. Layter, J. A. Appel, A. Kotlewski, W. Y. Lee, S. Stein and J. J. Thaler, Phys. Rev. D **7** (1973) 2565.
- [53] M. Gormley, E. Hyman, W. Y. Lee, T. Nash, J. Peoples, C. Schultz and S. Stein, Phys. Rev. D **2** (1970) 501.
- [54] F. Ambrosino *et al.* [KLOE collaboration], arXiv:0707.4137 [hep-ex].
- [55] T. Capussela [KLOE Collaboration], Acta Phys. Slov. **56** (2005) 341;
S. Giovannella *et al.* [KLOE Collaboration], 40th Rencontres de Moriond on QCD and High Energy Hadronic Interactions, La Thuile, Aosta Valley, Italy, 12-19 Mar 2005
arXiv:hep-ex/0505074.
- [56] W. B. Tippens *et al.* [Crystal Ball Collaboration], Phys. Rev. Lett. **87** (2001) 192001.
- [57] M. Bashkanov *et al.*, arXiv:0708.2014 [nucl-ex].
- [58] A. Abele *et al.* [Crystal Barrel Collaboration], Phys. Lett. B **417** (1998) 193.
- [59] D. Alde *et al.* [Serpukhov-Brussels-Annecy(LAPP) Collaboration], Z. Phys. C **25** (1984) 225 [Yad. Fiz. **40** (1984) 1447].
- [60] M. N. Achasov *et al.*, JETP Lett. **73** (2001) 451 [Pisma Zh. Eksp. Teor. Fiz. **73** (2001) 511].
- [61] B. V. Martemyanov and V. S. Sopov, Phys. Rev. D **71** (2005) 017501 [arXiv:hep-ph/0502023].
- [62] J. Bijnens, P. Dhonte and P. Talavera, JHEP **0401** (2004) 050 [arXiv:hep-ph/0401039].
- [63] D. B. Kaplan and A. V. Manohar, Phys. Rev. Lett. **56** (1986) 2004.
- [64] J. Bijnens and J. Prades, Nucl. Phys. B **490** (1997) 239 [arXiv:hep-ph/9610360].